

Stability of bulk and pseudomorphic epitaxial semiconductors and their alloys

A. A. Mbaye,* D. M. Wood, and Alex Zunger
 Solar Energy Research Institute, Golden, Colorado 80401
 (Received 21 May 1987)

The Landau-Lifshitz theory of structural phase transitions permits identification of distinct classes of ordered ternary structures $A_n B_{4-n} C_4$ ($n=0-4$) whose structural units are the $A_n B_{4-n} C$ clusters spanning all possible nearest-neighbor environments in $A_x B_{1-x} C$ pseudobinary semiconductor alloys. A detailed description of how disordered bulk or epitaxial alloys may be described as a superposition of such clusters is given. Using Landau-Lifshitz structures as examples, the very different energetics of bulk-versus-epitaxial (ordered or disordered) ternary phases are described and investigated quantitatively via a simple valence-force-field model and harmonic elasticity theory. Under epitaxial conditions on a substrate of lattice constant a_s , a tetragonal degree of freedom for a ternary ordered compound controls the curvature about the minimum of the energy $E(a_s)$, while cell-internal structural parameters control the minimum of E and hence stability. Stable bulk compounds when grown under epitaxial conditions may change in relative stability, permitting artificial stabilization of desired ordered phases. Exotic *ordered* ternary compounds unstable in bulk form (and hence not found in the bulk phase diagram) may become stable when epitaxy-induced strain is accommodated more successfully in the ternary than in the binary constituents; the occurrence of miscibility gaps and spinodal decomposition for *disordered* alloys may be similarly suppressed under epitaxial conditions. Relaxation of cell-internal structural parameters is found crucial to a quantitative theoretical description of the enthalpies of mixing of bulk- or epitaxially-grown disordered alloys.

I. INTRODUCTION

Our current understanding of chemical trends in the structure and stability of crystals¹ has been largely directed to the vast database of *bulk* materials, such as that compiled recently by Villars and Calvert.² Advances in *epitaxial* growth methods have pointed, however, to the possibility of equilibrium structural forms of semiconductors which do not appear in the equilibrium *bulk* phase diagrams of the same compounds. Such are, for example, rhombohedral^{3(a)} SiGe and^{3(b)} GaInAs₂, the famatinite forms⁴ of InGa₃As₄ and In₃GaAs₄, chalcopyritelike⁵ and CuAu-I-like⁵ forms of Ga₂AsSb, CuAu-I-like (tetragonal^{6(a)}) GaAlAs₂ and^{6(b)} InGaAs₂ (none of which are observed in the bulk phase diagram of Si_xGe_{1-x}, In_xGa_{1-x}As, GaAs_xSb_{1-x}, and Ga_xAl_{1-x}As, respectively), *cubic* epitaxial phases of⁷ CdS and⁸ SiC (observed at temperatures where the bulk phase diagrams show only hexagonal phases) and the α phase of Sn (not the normal β phase) observed⁹ to grow on InSb(110). It has similarly been noted¹⁰ that epitaxial lattice matching to a substrate can significantly perturb the solid composition from that mandated by the bulk equilibrium phase diagram, even permitting epitaxial growth of an alloy inside the bulk miscibility gap region (e.g.,¹¹ GaAs_{1-x}Sb_x). Similar epitaxy-induced phase stabilization effects were recently observed in metallurgy, e.g., ferromagnetic fcc (not bcc) Fe grown¹² on Cu(111), bcc (not fcc) Ni grown¹³ on Fe(001), ferromagnetic fcc (not hexagonal) Co grown^{14(a)} on Cu(001) or bcc Co grown^{14(b)} on GaAs, and bcc (not fcc) Ag grown on^{14(c)} InSb. Such epitaxy-induced structural stabilization has

been previously analyzed in terms of phenomenological elastic continuum models of substrate strain,^{10,15} but only recently¹⁶ has a microscopic (atomistic) model been advanced for the epitaxial SiGe system.³ In this paper we illustrate the general physical principles of epitaxial stabilization of tetrahedral adamantine semiconductor crystals using a simple valence-force-field method¹⁷ and the ternary Ga_nIn_{4-n}P₄ system as a prototypical example. A brief description of some of this work has already appeared.¹⁸

II. ORDERED LANDAU-LIFSHITZ ADAMANTINE STRUCTURES

The systems we will consider consist of two isovalent zinc-blende semiconductors AC and BC (specifically GaP and InP) and their mixtures. These mixtures can form, among others, a single-phase disordered alloy $A_x B_{1-x} C$, a two-phase (AC -rich and BC -rich) mixture, or ternary ordered compounds $A_n B_{4-n} C_4$ with $n=0, 1, 2, 3,$ and 4 . These ordered structures can be stable low-temperature phases of the alloy according to the general principles outlined by Landau and Lifshitz.^{19,20} The conditions for selecting such possible ground-state ordered phases of a face centered cubic (fcc) parent lattice with A - B , A - C , and B - C interactions are^{19,20} (i) the space group of the ordered structure must be a subgroup of that of the disordered alloy, and (ii) the possible ordered structure must be associated with an ordering vector located at a special \mathbf{k} point of the parent space group.¹⁹ These necessary conditions permit not only selection of the ordered structures but also their classification in families associated with the same star of

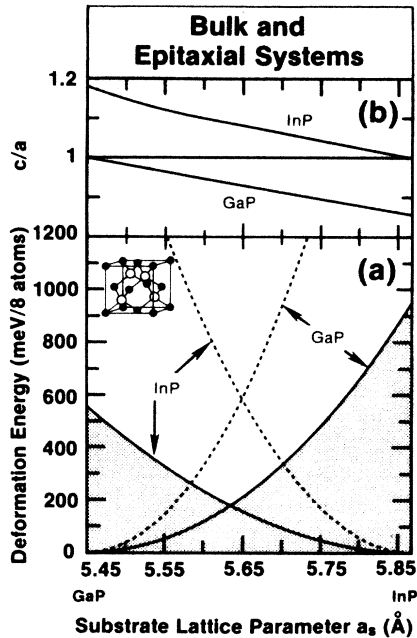


FIG. 1. Deformation energy of cubic (dashed lines) and tetragonally distorted epitaxial (solid lines) GaP and InP, (a), and dependence of c/a upon substrate lattice parameter a_s , (b). Shaded area indicates substrate strain. The inset shows the zinc-blende structure.

ordering vectors. There are eight such $A_nB_{4-n}C_4$ systems we wish to consider: for $n=0$ and 4 we have the binary end-point zinc-blende ($F\bar{4}3m$ space group) compounds AC and BC (inset to Fig. 1); for $n=2$ we have the 50%-50% compound ABC_2 with either a CuAu-I cation (A,B) sublattice⁶ [corresponding to the ordering

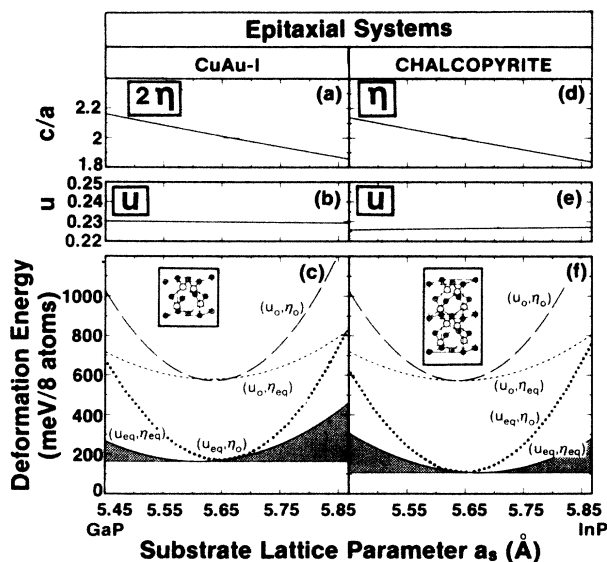


FIG. 2. Variation with substrate lattice parameter of structural parameters and deformation energies of epitaxial chalcopyrite and CuAu-I-like GaInP_2 ; insets show crystal structures. Deformation energies are shown for four different levels of relaxation: subscripts 0 and eq indicate undistorted and fully relaxed values, respectively. Shaded areas indicate substrate strain in the fully relaxed structures.

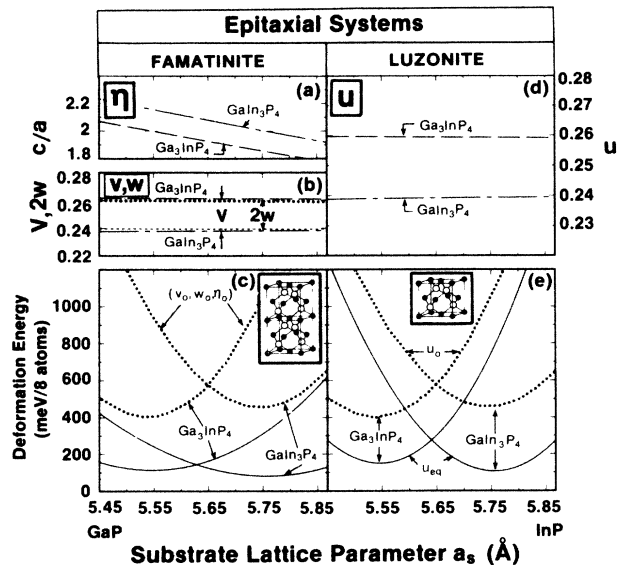


FIG. 3. Variation of structural parameters and deformation energies for epitaxial famatinite and luzonite GaIn_3P_4 and Ga_3InP_4 ; insets show crystal structures. Deformation energies are shown for two levels of structural relaxation: complete relaxation (solid lines) and the completely unrelaxed structures (dashed lines).

vector $\mathbf{k}_1 = (2\pi/a)(0,0,1)$, the $P\bar{4}2m$ structure shown in the inset to Fig. 2(c)] or the chalcopyrite (CP) structure⁵ ($I\bar{4}2d$) [corresponding to the ordering vector $\mathbf{k}_2 = (2\pi/a)(2,0,1)$, inset to Fig. 2(f)], whereas for $n=1$ and 3 we have the 25%-75% and 75%-25% compounds A_3BC_4 and AB_3C_4 , respectively, each appearing either in the "luzonite" (L) form ($P\bar{4}3m$) [corresponding to \mathbf{k}_1 , inset to Fig. 3(e)], or in the famatinite (F) form ($I\bar{4}2m$) [corresponding to \mathbf{k}_2 , inset to Fig. 3(c)]. Table I gives the translation vectors and atomic coordinates for these space groups. Most of the structures considered here actually occur in some minerals with tetrahedral coordination,^{21,22} e.g., the chalcopyrite form (CuFeS_2 , CuInSe_2 , etc.), the luzonite form²² (Cu_3AsS_4 or Cu_3VS_4), and the famatinite form (Cu_3AsSe_4 , Cu_3SbS_4 , Cu_3SbSe_4). Wurtzite analogs are also possible²¹ (e.g., Cu_3AsS_4 also exists in the hexagonal "energite" form), but will not be considered here.

A. Cell-external and cell-internal structural degrees of freedom

The structurally significant feature of these ternary $A_nB_{4-n}C_4$ phases, which distinguishes them from their binary constituents AC and BC , is that, whereas the latter have but a single structural degree of freedom in the zinc-blende form (the cubic lattice parameter a), the former have, in addition to two external degrees of freedom (the cell dimensions a and c , where the tetragonal ratio is denoted here as $\eta = c/a$; luzonite has $\eta=1$), some cell-internal degrees of freedom which control the position of the common atom C with respect to the fcc sites occupied by A and B . For example, in the CuAu-I structure² the two nearest-neighbor bond lengths can be expressed as

TABLE I. Primitive translation vectors and atomic coordinates [in Cartesian coordinates (x,y,z)] for the five fcc Landau-Lifshitz structures $A_n B_{4-n} C_4$.

Structure and space group	Primitive translation vectors	Atomic positions	
Zinc blende, $F\bar{4}3m$	$\mathbf{a}_1 = (0, \frac{1}{2}, \frac{1}{2})a$	$\tau_A = (0, 0, 0)a$	
	$\mathbf{a}_2 = (\frac{1}{2}, 0, \frac{1}{2})a$	$\tau_B = (\frac{1}{4}, \frac{1}{4}, \frac{1}{4})a$	
	$\mathbf{a}_3 = (\frac{1}{2}, \frac{1}{2}, 0)a$		
CuAu-I-like, $P\bar{4}m2$	$\mathbf{a}_1 = (\frac{1}{2}, \frac{1}{2}, 0)a$	$\tau_A = (0, 0, 0)a$	
	$\mathbf{a}_2 = (-\frac{1}{2}, \frac{1}{2}, 0)a$	$\tau_B = \left[0, \frac{1}{2}, \frac{\eta}{2}\right]a$	
	$\mathbf{a}_3 = (0, 0, \eta)a$	$\tau_{C1} = (\frac{1}{4}, \frac{1}{4}, \eta u)a$	$\tau_{C2} = [\frac{1}{4}, \frac{3}{4}, \eta(1-u)]a$
Chalcopyrite, $I\bar{4}2d$	$\mathbf{a}_1 = (1, 0, 0)a$	$\tau_{A1} = (0, 0, 0)a$	$\tau_{C1} = \left[u, \frac{1}{4}, \frac{\eta}{8}\right]a$
	$\mathbf{a}_2 = (0, 1, 0)a$	$\tau_{A2} = \left[0, \frac{1}{2}, \frac{\eta}{4}\right]a$	$\tau_{C2} = \left[1-u, \frac{3}{4}, \frac{\eta}{8}\right]a$
	$\mathbf{a}_3 = \left[\frac{1}{2}, \frac{1}{2}, \frac{\eta}{2}\right]a$	$\tau_{B1} = (\frac{1}{2}, \frac{1}{2}, 0)a$	$\tau_{C3} = \left[\frac{1}{4}, \frac{1}{2} + u, \frac{3\eta}{8}\right]a$
Famatinite $I\bar{4}2m$	$\mathbf{a}_1 = (1, 0, 0)a$	$\tau_{B2} = \left[\frac{1}{2}, 0, \frac{\eta}{4}\right]a$	$\tau_{C4} = \left[\frac{3}{4}, \frac{1}{2} - u, \frac{3\eta}{8}\right]a$
	$\mathbf{a}_2 = (0, 1, 0)a$	$\tau_{A1} = (\frac{1}{2}, \frac{1}{2}, 0)a$	$\tau_{C1} = (v, v, \eta w)a$
	$\mathbf{a}_3 = \left[\frac{1}{2}, \frac{1}{2}, \frac{\eta}{2}\right]a$	$\tau_{A2} = \left[0, \frac{1}{2}, \frac{\eta}{4}\right]a$	$\tau_{C2} = (1-v, 1-v, \eta w)a$
Luzonite, $P\bar{4}3m$	$\mathbf{a}_1 = (1, 0, 0)a$	$\tau_{A3} = \left[\frac{1}{2}, 0, \frac{\eta}{4}\right]a$	$\tau_{C3} = [\frac{1}{2} - v, \frac{1}{2} + v, \eta(\frac{1}{2} - w)]a$
	$\mathbf{a}_2 = (0, 1, 0)a$	$\tau_B = (0, 0, 0)a$	$\tau_{C4} = [\frac{1}{2} + v, \frac{1}{2} - v, \eta(\frac{1}{2} - w)]a$
	$\mathbf{a}_3 = (0, 0, 1)a$	$\tau_{A1} = (0, \frac{1}{2}, \frac{1}{2})a$	$\tau_{C1} = (u, u, u)a$
A_3BC_4 or AB_3C_4	$\mathbf{a}_2 = (0, 1, 0)a$	$\tau_{A2} = (\frac{1}{2}, 0, \frac{1}{2})a$	$\tau_{C2} = (u, 1-u, 1-u)a$
	$\mathbf{a}_3 = (0, 0, 1)a$	$\tau_{A3} = (\frac{1}{2}, \frac{1}{2}, 0)a$	$\tau_{C3} = (1-u, u, 1-u)a$
		$\tau_B = (0, 0, 0)a$	$\tau_{C4} = (1-u, 1-u, u)a$

$$R_{AC} = (\eta^2 u^2 + \frac{1}{8})^{1/2} a ;$$

$$R_{BC} = [\eta^2 (u - \frac{1}{2})^2 + \frac{1}{8}]^{1/2} a , \quad (1)$$

$$u \equiv \frac{1}{4} + [R_{AC}^2 - R_{BC}^2] / \eta^2 a^2 ,$$

and hence the degrees of freedom are $\{a, \eta, u\}$. The undistorted values of the structural parameters will be labeled with a subscript 0. For the CuAu-I-like structure $\eta_0 = 1$ and $u_0 = \frac{1}{4}$; hence the undistorted structure has $R_{AC}^0 = R_{BC}^0$. In the chalcopyrite structure² we have

$$R_{AC} = [u^2 + (4 + \eta^2) / 64]^{1/2} a ;$$

$$R_{BC} = [(u - \frac{1}{2})^2 + (4 + \eta^2) / 64]^{1/2} a , \quad (2)$$

$$u \equiv \frac{1}{4} + (R_{AC}^2 - R_{BC}^2) / a^2 ,$$

and hence the degrees of freedom are $\{a, \eta, u\}$; for the undistorted chalcopyrite structure $u_0 = \frac{1}{4}$, and $\eta_0 = 2$. In

the luzonite structure²

$$R_{AC} = [u^2 + 2(\frac{1}{2} - u)^2]^{1/2} a ;$$

$$R_{BC} = \sqrt{3}ua , \quad (3)$$

$$u \equiv \frac{1}{4} + (R_{BC}^2 - R_{AC}^2) / 2a^2 ,$$

and hence, the structural degrees of freedom are $\{a, u\}$; for the undistorted structure $u_0 = \frac{1}{4}$. The famatinite structure² has two internal degrees of freedom, w and v , producing bond lengths of the form

$$R_{A1,C} = [2(v - \frac{1}{2})^2 + \eta^2 w^2]^{1/2} a ,$$

$$R_{A2,C} = [(v - \frac{1}{2})^2 + v^2 + \eta^2 (w - \frac{1}{4})^2]^{1/2} a ,$$

$$R_{BC} = (2v^2 + \eta^2 w^2)^{1/2} a , \quad (4)$$

$$v \equiv \frac{1}{4} + (R_{BC}^2 - R_{A1,C}^2) / 2a^2 ,$$

$$w = \frac{1}{8} + [2(R_{BC}^2 - R_{A2,C}^2) - (R_{BC}^2 - R_{A1,C}^2)] / \eta^2 a^2,$$

the $A1-C$ ($A2-C$) bonds representing $\frac{1}{3}$ ($\frac{2}{3}$) of $A-C$ bonds present. Hence, the degrees of freedom are $\{a, \eta, v, w\}$; for the undistorted famatinite structure, $\eta_0 = 2$, $v_0 = \frac{1}{4}$, and $w_0 = \frac{1}{8}$.

B. Significance of cell-internal degrees of freedom for structural stability

When $\eta = \eta_0$ and the C atom is at the *center* of the tetrahedron formed by its A and B neighbors [i.e., $u = u_0$, $v = v_0$, and $w = w_0$ in Eqs. (1)–(4)] one has *equal* bond lengths $R_{AC}^0 = R_{BC}^0 = \sqrt{3}a/4$. These undistorted bond lengths are generally different from the “ideal” bond lengths $d_{AC}^0 = \sqrt{3}a_{AC}/4$ and $d_{BC}^0 = \sqrt{3}a_{BC}/4$ of the binary zinc-blende structures AC and BC , respectively. These differences, as well as the corresponding deviations from ideal tetrahedral bond angles $\theta^0 = 109.5^\circ$, set up a microscopic (cell-internal) strain energy proportional to $(\theta - \theta^0)^2$ and $(R_{\alpha\beta} - d_{\alpha\beta}^0)^2$. These systems must lower the microscopic strain energy resulting from this failure to accommodate ideal bond configurations by adjusting the *internal* degrees of freedom. The degree of strain energy lowering reflects the availability of suitable structural degrees of freedom, hence their crucial role in stabilizing *bulk* phases. As we will see below (Sec. IV), under pseudomorphic *epitaxial* conditions the cell dimensions parallel to the substrate are *externally fixed* by the substrate. Relative epitaxial stability is hence determined by relaxation of the *remaining* structural degrees of freedom, hence their significant role in epitaxial stability. This highlights the important difference between binary and ternary epitaxial systems: whereas in binaries a large epitaxial strain can be relieved only through a tetragonal deformation or by creation of misfit dislocations, in ternaries the system can also relax its internal structural parameters to reduce strain energy.

III. BULK PHASES

A. Enthalpies of formation of ordered bulk phases

The enthalpy of formation^{10,16,23} of ordered *bulk* $A_n B_{4-n} C_4$ compounds in structure type λ (chalcopyrite, CuAu-like, luzonite, famatinite) is given by the difference of the total energy $E^{(\lambda,n)}$ of the ternary compound when all of its degrees of freedom attain their energy-minimizing equilibrium (eq) values, and the energy of equivalent amounts of its binary end-point compounds, also at equilibrium. The volume-dependent total energy $E^{(\lambda,n)}(V)$ of a given ordered compound (λ, n) is obtained by finding for each cell volume V the values of the cell-external [lattice parameter $a(V)$ and $\eta(V)$] and cell-internal degrees of freedom u, v, w [denoted collectively as $\{u(V)\}$] which minimize the energy. This produces the equation of state

$$E^{(\lambda,n)}(V) = E^{(\lambda,n)}(A_n B_{4-n} C_4, V, a(V), \eta(V), \{u(V)\}). \quad (5)$$

The formation enthalpy of the ordered phase (λ, n) is hence defined (per eight atoms) as

$$\Delta H^{(\lambda,n)} = E_{\text{eq}}^{(\lambda,n)}(A_n B_{4-n} C_4, V_{\text{eq}}^{(\lambda,n)}) - nE(AC, a_{AC}) - (4-n)E(BC, a_{BC}), \quad (6)$$

where all parameters not denoted explicitly are taken at equilibrium. Note that positive (negative) $\Delta H^{(\lambda,n)}$ reflects instability (stability) of $A_n B_{4-n} C_4$ towards disproportionation into $nAC + (4-n)BC$ at $T=0$.

In order to establish the extent to which the relaxation of certain structural parameters lowers the strain energy, one can repeat the above relaxation process, keeping certain variables fixed at their undistorted values. For example, keeping $u = u_0$ and $\eta = \eta_0$ produces the “unrelaxed” deformation energy $E_{u_0, \eta_0}^{(\lambda,n)}(V)$. Similarly, one can calculate at $u = u_{\text{eq}}$ but $\eta = \eta_0$ the energy $E_{\eta_0}^{(\lambda,n)}(V)$, or at $u = u_0$ and $\eta = \eta_{\text{eq}}$ the energy $E_{u_0}^{(\lambda,n)}(V)$. Each of the partially relaxed energies could be used in analogy with Eq. (6) to define a partially relaxed formation enthalpy. These will be used to assess the relative significance of various structural degrees of freedom in lowering the formation enthalpies.

B. Mixing enthalpies and bond lengths of disordered bulk alloys

1. General results

Since a disordered alloy $A_x B_{1-x} C$ contains a statistical mixture of several local environments, its enthalpy of mixing

$$\Delta H^D(x) \equiv H^D(A_x B_{1-x} C) - xH(AC) - (1-x)H(BC) \quad (7)$$

can be approximately expressed^{23,24} as a corresponding mixture of cluster energies $\Delta E^{(\lambda,n)}$, which we take from *ordered* compounds in which they exist in pure form. (We drop for convenience the index λ ; its choice will be specified in Sec. VII.) Denoting by $V_{\text{eq}}^{(n)}$ the equilibrium volume of ordered structure n , its excess energy function (relative to equivalent amounts of AC and BC at their equilibrium) can be written as

$$\Delta E^{(n)}(V) = \Delta H^{(n)} + F_n^b(V - V_{\text{eq}}^{(n)}), \quad (8)$$

where $\Delta H^{(n)}$ is the value at the minimum [Eq. (6)] and $F_n^b(V)$ describes the energy associated with volume deformations of the bulk phase (b) around the minimum. $F_n^b(V)$ could be obtained by fitting the numerical data $\Delta E^{(n)}(V)$ obtained from total energy calculations. For purposes of illustration we may use the harmonic form

$$F_n^b(V) \simeq \frac{B_n}{2V_{\text{eq}}^{(n)}(X_n)} (V - V_{\text{eq}}^{(n)})^2, \quad (9)$$

where $V_{\text{eq}}^{(n)} = V_{\text{eq}}^{(n)}(X_n)$ is the equilibrium volume of the ordered structure $A_n B_{4-n} C_4$ at its stoichiometric com-

position $x = X_n = n/4$ and B_n is the bulk modulus of ordered phase n . The excess energy of the disordered (D) alloy at composition x and temperature T can be approximated^{23,24} as a superposition of cluster energies as

$$\Delta E(V) = \sum_n P_n(x, T) \Delta E^{(n)}(V), \quad (10)$$

where $P_n(x, T)$ ($n=0-4$) is the occurrence probability of the local environment n at (x, T) . To find the relation-

ship between equilibrium alloy volume and its composition x , one imposes for applied external pressure Π

$$\left. \frac{\partial \Delta E^D(V)}{\partial V} \right|_x = -\Pi = \sum_n P_n(x, T) \frac{\partial F_n^b(V)}{\partial V}, \quad (11)$$

yielding the equilibrium alloy volume $V_{\text{eq}}(x)$ (including possible deviations from Vegard's rule). Using the harmonic form Eq. (9) this gives

$$V_{\text{eq}}(x) = \left[-\Pi + \sum_n P_n(x, T) B_n \right] / \sum_n P_n(x, T) [B_n / V_{\text{eq}}^{(n)}(X_n)], \quad (12)$$

so if the parameters $\{B_n, V_{\text{eq}}^{(n)}\}$ of the ordered phases and the cluster probabilities $P_n(x, T)$ are known, $V_{\text{eq}}(x)$ can be calculated. Substituting $V_{\text{eq}}(x)$ for V in Eq. (10) then gives the mixing enthalpy of the disordered (D) alloy

$$\begin{aligned} \Delta H^D(x, T) &= \Delta E^D[V_{\text{eq}}(x)] \\ &= \sum_n P_n(x, T) \Delta E^{(n)}[V_{\text{eq}}(x)]. \end{aligned} \quad (13)$$

Using Eqs. (8) and (13) we obtain

$$\begin{aligned} \Delta H^D(x, T) &= \sum_n P_n(x, T) \Delta H^{(n)} \\ &+ \sum_n P_n(x, T) F_n^b [V_{\text{eq}}(x) - V_{\text{eq}}^{(n)}]. \end{aligned} \quad (14)$$

For a perfectly ordered phase n , $x = X_n$, $V_{\text{eq}}(x) = V_{\text{eq}}^{(n)}(X_n)$, and $P_m(x, T) = \delta_{m,n}$; hence $\Delta H^D(x, T)$ becomes $\Delta H^{(n)}$. As discussed in Sec. VIB, for such ordered phases $\Delta H^{(n)}$ should be computed by relaxing all structural degrees of freedom $\{u, \eta\}$ for each ordered phase. This is also true for the clusters describing the disordered phase.

2. Alloy-induced cluster relaxation

It is possible that in the alloy environment certain equilibrium properties of the clusters $A_n B_{4-n}$ change²⁵ with respect to their values in the pure ordered compound $A_n B_{4-n} C_4$. Replacing a given B atom by a single A atom in the zinc-blende BC crystal, for example, will create an AB_3C cluster in addition to the B_4C clusters of the "host." The energy $\Delta E^{(1)}$ of AB_3C embedded in the BC medium may differ from the energy of this cluster in the pure ordered compound AB_3C_4 . An extremely useful means of accounting for this "alloy-induced cluster relaxation" is to permit the equilibrium volume $V_{\text{eq}}^{(n)}(x)$ of cluster n in the alloy to deviate from its value $V_{\text{eq}}^{(n)}(X_n)$ in the pure ordered phase²⁵ (where $x = X_n$). To first order in a Taylor expansion, the equilibrium volume of cluster n in the alloy [$V_{\text{eq}}^{(n)}$ of Eq. (14)] can be written

$$V_{\text{eq}}^{(n)}(x) = V_{\text{eq}}^{(n)}(X_n) + K_n^b [V_{\text{eq}}(x) - V_{\text{eq}}^{(n)}(X_n)] + \dots, \quad (15)$$

where K_n^b are relaxation constants for the bulk (b) alloy. If $K_n^b = 0$ (no alloy-induced cluster relaxation) $V_{\text{eq}}^{(n)}(x) = V_{\text{eq}}^{(n)}(X_n)$ for all x . [This is analogous to the frequently made assumption that an atom has a characteristic size (or molar volume) independent of its chemical environment.] If $K_n^b = 1$ (complete relaxation) all clusters have the same equilibrium volumes as the alloy, i.e., $V_{\text{eq}}^{(n)}(x) = V_{\text{eq}}(x)$. (This alloy-induced cluster relaxation is a construct for including "effective alloy medium" effects on cluster *energies* only.)

If for simplicity all K_n^b are taken as a constant K^b , $V_{\text{eq}}(x)$ remains the same (for zero pressure Π) as given in Eq. (12). The mixing enthalpy is obtained by using $V_{\text{eq}}^{(n)}(x)$ of Eq. (15) in Eq. (14). Defining, in the harmonic approximation,

$$h_{\text{bulk}}^D(x, T) \equiv \sum_n P_n(x, T) \frac{B_n}{2V_{\text{eq}}^{(n)}(X_n)} [V_{\text{eq}}(x) - V_{\text{eq}}^{(n)}(X_n)]^2, \quad (16)$$

the mixing enthalpy can be written

$$\begin{aligned} \Delta H^D(x, T) &= \left[\sum_n P_n(x, T) \Delta H^{(n)} + h_{\text{bulk}}^D(x, T) \right] \\ &+ K^b (K^b - 2) h_{\text{bulk}}^D(x, T), \end{aligned} \quad (17)$$

where the term in large parentheses is the mixing enthalpy without alloy-induced cluster relaxation (but for which all cluster energies are minimized with respect to the structural parameters of the ordered compound from which they are taken), while the last term (negative, since $K^b \leq 1$) is the correction due to alloy-induced cluster relaxation.

In what follows, we will approximate $P_n(x, T)$ as the *random* probabilities

$$P_n^R(x) = \binom{4}{n} x^n (1-x)^{4-n} \quad (18)$$

appropriate in the high-temperature limit, since observed mixing enthalpies for semiconductor alloys are extracted from high-temperature liquidus-solidus data.²⁶ Calculations with *variational* probabilities (obtained in the cluster variation method) are reported for $\text{Ga}_x\text{In}_{1-x}\text{P}$ in Ref. 24, but for purposes of contrasting general trends in

bulk versus epitaxial growth, random probabilities [Eq. (18)] are sufficient. The observed mixing enthalpies at high-temperature are customarily represented as^{26,27}

$$\Delta H^D(x) \equiv \Omega x(1-x) \quad (19)$$

where Ω , independent of temperature in this limit, is the "interaction parameter." Using Eq. (17) we may write

$$\Omega = \frac{\Delta H^D(x, T)}{x(1-x)} = \Omega_1 + \Omega_2 + \Omega_3, \quad (20)$$

where the contribution from the bulk formation enthalpies is

$$\Omega_1 = \sum_n P_n(x) \Delta H^{(n)} / x(1-x), \quad (21)$$

the contribution of cluster strain is

$$\Omega_2 = h_{\text{bulk}}^D(x) / x(1-x), \quad (22)$$

and the alloy-induced cluster relaxation contribution is

$$\Omega_3 = K^b(K^b - 2)h_{\text{bulk}}^D(x) / x(1-x). \quad (23)$$

In Sec. VII B we will calculate $\Delta H^D(x)$ of Eq. (17) and assess the relative importance of its three contributions [Eqs. (21)–(23)].

3. Bond lengths in disordered bulk alloy

In analogy with Eq. (10), the local nearest-neighbor atomic environment in a disordered fcc alloy involves all statistical possibilities spanned by the Landau-Lifshitz ordered structures^{20,23} ($A_n B_{4-n} C_4$): the C atom may be coordinated by A atoms only, forming an $A_4 C$ cluster ($n=4$), by $A_3 B$ ($n=3$), $A_2 B_2$ ($n=2$), AB_3 ($n=1$), or by B atoms only, forming $B_4 C$ ($n=0$). We then have the following average bond lengths in the disordered (D) phase:

$$R_{AC}^D(x) = \sum_n \omega_{AC}^{(n)} P_n(x, T) R_{AC}^{(n)} [V_{\text{eq}}(x)] / \sum_n \omega_{AC}^{(n)} P_n(x, T), \quad (24)$$

$$R_{BC}^D(x) = \sum_n \omega_{BC}^{(n)} P_n(x, T) R_{BC}^{(n)} [V_{\text{eq}}(x)] / \sum_n \omega_{BC}^{(n)} P_n(x, T),$$

where $R_{\alpha\beta}^{(n)} [V_{\text{eq}}(x)]$ is the equilibrium α – β bond length in structure type n for unit cell volume $V_{\text{eq}}(x)$ and $\omega_{\alpha\beta}^{(n)}$ is the number of α – β bonds in the structure n .

IV. EPITAXIAL PHASES

A. Enthalpies of formation of ordered epitaxial phases

When an $A_n B_{4-n} C_4$ compound is grown *epitaxially* in a dislocation-free, pseudomorphic fashion on a substrate (s) with lattice parameter a_s perpendicular to the growth direction, its lattice parameter a_{\parallel} parallel to the substrate is constrained²⁸ to equal a_s . Its energy is hence no longer given by Eq. (5); instead, one determines it by fixing the *lattice parameter* $a_{\parallel} = a_s$ (not the volume), and relaxing all other structural parameters. Denoting epitaxial energies by a tilde, this gives, in analogy with Eq. (5),

$$\tilde{E}^{(\lambda, n)}(a_s) = E^{(\lambda, n)}(A_n B_{4-n} C_4, a_s, c(a_s), \{u(a_s)\}). \quad (25)$$

In analogy with the bulk case (Sec. III A), one can define partially relaxed energies for epitaxial systems, by keeping certain structural parameters fixed.

Under pseudomorphic epitaxial conditions, the products (AC and BC) of a disproportionation reaction are also constrained to match a_s in the directions parallel to the substrate and will hence develop tetragonal distortions. The *epitaxial* formation enthalpy of the ordered compound (λ, n) grown on a substrate with $a_{\parallel} = a_s$ is¹⁶ (per eight atoms)

$$\begin{aligned} \delta H^{(\lambda, n)}(a_s) = & \tilde{E}^{(\lambda)}(A_n B_{4-n} C_4, a_{\parallel} = a_s) \\ & - n \tilde{E}(AC, a_{\parallel} = a_s) \\ & - (4-n) \tilde{E}(BC, a_{\parallel} = a_s). \end{aligned} \quad (26)$$

The restriction of the lattice parameter to a fixed value a_s costs strain energy. We define this substrate strain (ss) energy¹⁶ for the compound of structure type λ as the difference between the constrained and unconstrained ("free-floating") energies,

$$\begin{aligned} W_{\text{ss}}^{(\lambda, n)}(a_s) = & \tilde{E}^{(\lambda)}(A_n B_{4-n} C_4, a_{\parallel} = a_s) \\ & - E^{(\lambda)}(A_n B_{4-n} C_4; a_{\text{eq}}^{(n)}) \end{aligned} \quad (27)$$

(where all structural degrees of freedom not enumerated explicitly in the equations are again taken to be their equilibrium values for the relevant a_s).

Harmonic elasticity theory provides insight into the very different effects of constrained and unconstrained growth. For a hydrostatically deformed *cubic* material of equilibrium unit cell volume a_{eq}^3 the strain energy (per unit cell) may be written $E \simeq E(a_{\text{eq}}) + 9B a_{\text{eq}} (a - a_{\text{eq}})^2 / 2$, where the cubic bulk modulus is $B = (C_{11} + 2C_{12}) / 3$. In the presence of epitaxy-induced tetragonal distortions, however, *provided* a tetragonal distortion is permitted in the structural description of the crystal, one may minimize the elastic energy with respect to tetragonal distortion for fixed epitaxial strain, finding

$$W_{\text{ss}} = 9B_{\text{eff}} a_{\text{eq}} (a_s - a_{\text{eq}})^2 / 2, \quad (28)$$

where for the particular case of the [001] substrate orientation which we consider in detail here,

$$B_{\text{eff}} = 2\sigma_{100} / 9 = 2B(1 - C_{12} / C_{11}) / 3, \quad (29)$$

and $\sigma_{100} = C_{11} + C_{12} - 2C_{12}^2 / C_{11}$. (For other substrate orientations B_{eff} will depend differently on the elastic constants.²⁹) Since for typical III-V zinc-blende compounds¹⁸ $B / B_{\text{eff}} \sim 2.5 - 3$ (see Table II below), this analysis implies a pronounced reduction in curvature of the $\tilde{E}^{(\lambda, n)}(a_s)$ curves [Eq. (25)] about the global equilibrium value a_{eq} for tetragonally distorted epitaxial (as compared to bulk cubic) binary structures. To the extent that an ordered *ternary* compound may be described by cubic elastic constants, this analysis will also hold for ternary compounds. Alone among the ternary structures we consider, luzonite lacks a tetragonal degree of free-

TABLE II. Calculated minimum (min) energy lattice parameter (a_{\min}) in Å and deformation energy (in meV per eight atoms) for bulk and epitaxial ordered $\text{Ga}_n\text{In}_{4-n}\text{P}_4$ compounds. Here unrelaxed refers to $u = u_0$ and $\eta = \eta_0$. η relaxation refers to $u = u_0$ and $\eta = \eta_{\text{eq}}$; u relaxation refers to $\eta = \eta_0$ and $u = u_{\text{eq}}$, and “full relaxation” refers to u_{eq} and η_{eq} . Elastic moduli B and B_{eff} are in GPa.

System	Unrelaxed		η Relaxation		u Relaxation		Full relaxation		$B^{(n,\lambda)}$ (bulk)	$B_{\text{eff}}^{(n,\lambda)}$ (epitaxial)
	a_{\min}	Min of $\tilde{E}_{u_0\eta_0}(V)$ or $E_{u_0\eta_0}(V)$	a_{\min}	Min of $\tilde{E}_{u_0}(a)$ or $E_{u_0}(V)$	a_{\min}	Min of $\tilde{E}_{\eta_0}(a)$ or $E_{\eta_0}(V)$	a_{\min}	Min of $\tilde{E}(a)$ or $E(V)$		
GaP (ZB)	5.450	0.0	5.450	0.0	5.450	0.0	5.450	0.0	92.7	33.0
Ga_3InP_4 (L)	5.539	403.6	5.539	403.6	5.546	147.4	5.546	147.4	89.3 ^a	89.0 ^a
Ga_3InP_4 (F)	5.539	403.6	5.538	403.5	5.546	110.5	5.550	110.3	89.2	30.0
GaInP_2 (CuAu)	5.636	571.7	5.632	571.6	5.648	171.5	5.611	161.3	85.0	27.0
GaInP_2 (CP)	5.636	571.7	5.639	571.6	5.649	108.1	5.673	104.9	85.0	26.9
GaIn_3P_4 (L)	5.746	456.9	5.746	456.9	5.756	103.7	5.756	103.7	81.0 ^a	80.8 ^a
GaIn_3P_4 (F)	5.746	456.9	5.746	456.9	5.757	78.6	5.760	78.4	81.0	23.9
InP (ZB)	5.866	0.0	5.866	0.0	5.866	0.0	5.866	0.0	77.1	20.6

^aDifference reflects different harmonic regimes of $E(a)$ and $E(V)$.

dom η , so that under epitaxial conditions the curvature of its curve $\tilde{E}(a_s)$ is expected to be described by B rather than B_{eff} .

We see that the relative stabilities of epitaxial and bulk forms are given (per eight atoms) by the *excess* substrate strain energy, i.e., the difference between Eq. (26) and Eq. (6),

$$\begin{aligned} \Delta E_{\text{ss}}^{(\lambda,n)}(a_s) &\equiv \delta H^{(\lambda,n)}(a_s) - \Delta H^{(\lambda,n)} \\ &= W_{\text{ss}}^{(\lambda)} [A_n B_{4-n} C_4, a_s] - n W_{\text{ss}} [AC, a_s] \\ &\quad - (4-n) W_{\text{ss}} [BC, a_s]. \end{aligned} \quad (30)$$

Whereas the epitaxial restriction $a_{\parallel} = a_s$ necessarily raises the energies of AC , BC , and $A_n B_{4-n} C_4$ relative to the unrestricted (bulk) equilibrium values, it is possible that such an epitaxial constraint raises the energy of the binary constituents AC and BC even more than that of $A_n B_{4-n} C_4$ (since the former structures lack internal degrees of freedom), resulting in *epitaxial stabilization* when $\Delta E_{\text{ss}}^{(\lambda,n)} < 0$. Using Eqs. (26) and (28), a simple harmonic model would predict (per eight atoms) for $A_n B_{4-n} C_4$

$$\begin{aligned} \Delta E_{\text{ss}}^{(n)}(a_s) &= \delta H^{(n)}(a_s) - \Delta H^{(n)} \\ &= + \frac{9}{2} \left[B_{\text{eff}}^{(n)} a_{\text{eq}}^{(n)} (a_s - a_{\text{eq}}^{(n)})^2 \right. \\ &\quad \left. - \frac{n}{4} B_{\text{eff}}^{AC} a_{AC} (a_s - a_{AC})^2 \right. \\ &\quad \left. - \frac{(4-n)}{4} B_{\text{eff}}^{BC} a_{BC} (a_s - a_{BC})^2 \right]. \end{aligned} \quad (31)$$

For $a_s = a_{\text{eq}}^{(n)}$ it is obvious that $\delta H^{(n)} - \Delta H^{(n)} < 0$, so that the epitaxial compound has been stabilized with respect to its bulk counterpart. We will find in Sec. VI C that in fact $\delta H^{(n)}(a_s) < 0$ for most of the range $a_{AC} < a_s < a_{BC}$ for all epitaxial ternary compounds except luzonite.

Furthermore, the availability of different structural degrees of freedom in different ordered compounds can

make one more adaptable to the epitaxial constraint than another, leading to *epitaxial selectivity* between different structures $\{\lambda\}$ of the same composition n . We will refer to this phenomenon as “epitaxial selection of species,” with obvious analogies to Darwin’s viewpoint.

B. Mixing enthalpies and bond lengths of disordered epitaxial alloys

When an alloy $A_x B_{1-x} C$ is grown epitaxially on a substrate with lattice parameter a_s parallel to the growth direction, its excess energy is given, in analogy with the bulk case of Eq. (10), by

$$\Delta E^D(c, a_s) = \sum_n P_n(x, T) \Delta E^{(n)}(c, a_s), \quad (32)$$

where $\Delta E^{(n)}(c, a_s)$ is the epitaxial excess energy function for cluster n [with respect to its epitaxially constrained binary constituents, as in Eq. (26)]. The equilibrium value $c_{\text{eq}}^{(n)}$ of the tetragonal dimension c for ordered structure n grown on an [001] substrate of lattice constant a_s is determined by the condition $\partial \Delta E^{(n)}(c, a_s) / \partial c = 0$. For fixed a_s the harmonic approximation³⁰ yields

$$c_{\text{eq}}^{(n)}(a_s) = a_{\text{eq}}^{(n)} - 2 \frac{C_{12}^{(n)}}{C_{11}^{(n)}} (a_s - a_{\text{eq}}^{(n)}). \quad (33)$$

Writing

$$\Delta E^{(n)}(c, a_s) = \delta H^{(n)}(a_s) + F_n^{\text{epi}} [c - c_{\text{eq}}^{(n)}(a_s)] \quad (34)$$

[analogous to Eq. (8) for the bulk case], in the harmonic case³⁰ per eight atoms

$$F_n^{\text{epi}} [c - c_{\text{eq}}^{(n)}(a_s)] \approx \frac{1}{2} C_{11}^{(n)} a_{\text{eq}}^{(n)}(X_n) [c - c_{\text{eq}}^{(n)}(a_s)]^2 \quad (35)$$

[analogous to Eq. (9)]. A variational determination of the epitaxial alloy’s equilibrium tetragonal dimension $c_{\text{eq}}(x)$ [analogous to the determination of $V_{\text{eq}}(x)$ for a bulk alloy] may also be carried out. Since a_s is fixed by

choice of substrate, we impose the condition of zero perpendicular stress,

$$\left. \frac{\partial \Delta E(c, a_s)}{\partial c} \right|_{x, a_s} = 0, \quad (36)$$

yielding, in analogy with Eq. (12) for the bulk case,

$$c_{\text{eq}}(a_s, x) = \frac{\sum_n P_n(x, T) C_{11}^{(n)} a_{\text{eq}}^{(n)} c_{\text{eq}}^{(n)}(a_s)}{\sum_n P_n(x, T) C_{11}^{(n)} a_{\text{eq}}^{(n)}}. \quad (37)$$

Inserting $c_{\text{eq}}(a_s, x)$ into Eq. (32) and using Eq. (34), we may write the epitaxial mixing enthalpy as

$$\begin{aligned} \delta H^D(a_s, x, T) &= \Delta E[c_{\text{eq}}(a_s, x)] \\ &= \sum_n P_n(x, T) \delta H^{(n)}(a_s) \\ &\quad + \sum_n P_n(x, T) F_n^{\text{epi}}[c_{\text{eq}}(x, a_s)]. \end{aligned} \quad (38)$$

As described in Eqs. (15) and (17) for the bulk case, the effects of alloy-induced cluster relaxation may be included by the construction

$$a_{\text{eq}}^{(n)}(x) = a_{\text{eq}}^{(n)}(X_n) + K_n^{\text{epi}}[a_{\text{eq}}(x) - a_{\text{eq}}^{(n)}(X_n)] \quad (39)$$

(with analogous expressions for other cell dimensions for noncubic ordered compounds). We note that even in the epitaxially constrained alloy cluster relaxation is toward the global alloy equilibrium lattice constant $a_{\text{eq}}(x)$ and does not depend on a_s . Examination of the case $a_s = a_{\text{eq}}(x)$ (an epitaxial alloy grown on a substrate whose lattice constant is the equilibrium value of the bulk alloy, so that there is no epitaxial constraint) demonstrates that, in comparing a bulk system (relaxation constant K^b) and an epitaxial one (relaxation constant K^{epi}) one must have $K^{\text{epi}} = K^b$.

Using Eq. (30), we see that Eq. (38) gives

$$\begin{aligned} \delta H^D(a_s, x, T) &= \sum_n P_n(x, T) \{ \Delta H^{(n)} + F_n^{\text{epi}}[c_{\text{eq}}(a_s, x)] \} \\ &\quad + \sum_n P_n \Delta E_{\text{ss}}^{(n)}(a_s). \end{aligned} \quad (40)$$

The discussion following Eq. (31) demonstrated that $\Delta E_{\text{ss}}^{(n)}(a_s) < 0$ is likely for at least part of the range $a_{AC} < a_s < a_{BC}$, so that we expect the epitaxial constraint to lower the mixing enthalpy of the disordered alloy. To illustrate the consequences, consider a bulk $A_x B_{1-x} C$ alloy which exhibits a miscibility gap, i.e., for which (inside this gap) a two-phase (AC - and BC -rich) mixture is of lower free energy than a homogeneous single-phase disordered alloy. When grown epitaxially on a substrate lattice matched to the bulk disordered alloy, there will be no effect on the single-phase alloy. The disproportionation products (AC - and BC -rich), however, are *not* lattice matched to the substrate, and the associated strain energy raises, under epitaxial conditions, the free energy of the two-phase system. Hence, whereas in *bulk* form the two-phase system had the lowest free energy, under *epitaxial* conditions the single-phase disordered al-

loy has lower free energy. If, in addition, an *ordered* bulk compound has lower free energy than the bulk single-phase alloy (the commonly encountered situation, (see Sec. VII B and figures therein below), under epitaxial conditions such an ordered phase will have the lowest free energy. The average $A-C$ and $B-C$ bond lengths in the epitaxial alloys are calculated in analogy with the bulk case of Eq. (24) with the substitution $R_{\alpha\beta}^{(n)}[V_{\text{eq}}(x)] \rightarrow R_{\alpha\beta}^{(n)}[a_s, c_{\text{eq}}(x)]$.

V. MODELING THE ENERGIES OF ORDERED COMPOUNDS

In general, the enthalpy of formation $\Delta H^{(\lambda, n)}$ of a given ordered structure contains two types of contributions:^{16,23,24,27} *First*, if one assumes that the elastic properties of bonds in the ternary compound are unchanged relative to those in the binary constituents, the formation enthalpy contains a contribution $\Delta E_{\text{ms}}^{(\lambda, n)}$ due to microscopic strain (ms), reflecting the failure of the structure to accommodate the ideal bond lengths and angles of the binary constituents. Were these structures topologically unconstrained¹⁶ (i.e., they possessed sufficient degrees of freedom to make all bond lengths and angles ideal, as is the case for the binary zinc-blende or the rhombohedral structures¹⁶), we would have $\Delta E_{\text{ms}}^{(\lambda, n)} \equiv 0$; otherwise, $\Delta E_{\text{ms}}^{(\lambda, n)} > 0$. The *second* contribution to the enthalpy of formation of an ordered compound can be thought of as “chemical,” incorporating actual interactions (e.g., charge transfer) between AC and BC in $A_n B_{4-n} C_4$, neglected in the previous step. The evaluation of this $\Delta E_{\text{chem}}^{(\lambda, n)}$ requires a quantum-mechanical calculation. Such calculations have been recently reported for GaP-InP,^{23,24} Si-Ge,^{16,20} Si-C,^{16,20} GaAs-AlAs,³¹ CdTe-HgTe,³² and MnTe-CdTe.³²

The total formation enthalpy is hence

$$\Delta H^{(\lambda, n)} = \Delta E_{\text{ms}}^{(\lambda, n)} + \Delta E_{\text{chem}}^{(\lambda, n)}. \quad (41)$$

Stable ($\Delta H^{(\lambda, n)} < 0$) ordered ternary structures of the $A_n B_{4-n} C_4$ form²¹ usually contain atoms A and B from *different* columns of the Periodic Table (e.g., chalcopyrite compounds $A^{\text{I}} B^{\text{III}} C_2^{\text{VI}}$, pnictide compounds $A^{\text{II}} B^{\text{IV}} C_2^{\text{V}}$, or famatinitelike compounds $A^{\text{I}} B^{\text{V}} C_4^{\text{VI}}$). In these *heterovalent* compounds one finds that $\Delta H^{(\lambda, n)} \ll 0$ (a few eV per mole), primarily because of strong electrostatic interactions which render $\Delta E_{\text{chem}}^{(\lambda, n)}$ strongly negative. There is a special class of $A_n B_{4-n} C_4$ adamantine compounds—those we consider in this paper—in which the dissimilar elements A and B are *isovalent* (i.e., belong to the same column in the periodic table). In this class of compounds (“pseudobinaries,” e.g., $A_n^{\text{III}} B_{4-n}^{\text{III}} C_4^{\text{V}}$ or $A_n^{\text{II}} B_{4-n}^{\text{II}} C_4^{\text{VI}}$) there are only weak electrostatic energies; hence $\Delta H^{(\lambda, n)}$ is about 2 orders of magnitude smaller^{23,24} than in the corresponding *heterovalent* adamantine compounds; only recently have isovalent ordered ternary compounds been prepared³⁻⁶ (their $\Delta H^{(\lambda, n)}$ are not known experimentally). Self-consistent total energy calculations reveal rather small (negative or positive) values for $\Delta H^{(\lambda, n)}$ in such isovalent compounds, e.g., for GaAlAs₂ in the CuAu-I-like structure³¹ $\Delta H^{(2)} \simeq +10$ meV/atom-pair, for ferromagnetic CdMnTe₂ (Ref. 32) in

the same structure $\Delta H^{(2)} = -25$ meV/atom-pair, for CdHgTe₂ (Ref. 32) $\Delta H^{(2)} = +6.1$ meV/atom-pair, for zinc-blende SiGe (Refs. 16 and 20) $\Delta H = +17.8$ meV/pair but for SiC in the same structure^{16,20} $\Delta H = -659$ meV/pair (+0.23, -0.58, +0.14, +0.41, and -15.2 kcal/atom-pair, respectively). Whereas *ordered* isovalent compounds have small (negative or positive) $\Delta H^{(\lambda,n)}$, the corresponding *disordered* isovalent alloys are known to all have *positive* enthalpies of formation¹⁰ $\Delta H^D(x)$, of order 0–130 meV/atom-pair (0–3 kcal/mole).

It has previously been observed²³ that, whereas in isovalent compounds the *value* of $\Delta H^{(\lambda,n)}$ is affected both by “strain” and chemical effects [Eq. (41)], the bulk equilibrium *geometry* [minimizing $E^{(\lambda,n)}(V)$ of Eq. (5)] is decided primarily by the strain energy. Since, furthermore, in this work we are interested primarily in the *relative* stabilities of bulk and epitaxial forms of isovalent ternary semiconductors, we will consider, for purposes of illustration, only the microscopic strain energy $\Delta E_{ms}^{(\lambda,n)}$ in Eq. (41). We hence use Keating’s¹⁷ valence-force-field (VFF) model for the deformation energy $E^{(\lambda,n)}[V, a, \eta, \{u\}]$, i.e. (for the adamantite tetrahedrally coordinated compounds we consider),

$$E = \sum_{i=1}^{2n_b} \frac{3}{8d_i^2} \alpha_i (\mathbf{r}_i \cdot \mathbf{r}_i - d_i^2)^2 + \sum_{j=1}^{6n_b} \frac{3}{8d_j^{(1)}d_j^{(2)}} \beta_j (\mathbf{r}_j^{(1)} \cdot \mathbf{r}_j^{(2)} + \frac{1}{3}d_j^{(1)}d_j^{(2)})^2, \quad (42)$$

where in the first sum (which runs over all distinct bonds in the unit cell, $2n_b$ is in number if there are n_b atoms in the basis, since each atom is fourfold coordinated) d_i is the ideal bond length (i.e., that of the binary) and α_i is the bond stretching force constant^{17,27} for bond i . Since each atom in the cell participates in 12 bond angles, the second sum runs over the $6n_b$ distinct angles in the unit cell. In the second sum β_j is the bond-bending force constant²⁷ for bond angle j , $\mathbf{r}_j^{(1)}$ is the vector from the central atom along one arm of the angle, and $\mathbf{r}_j^{(2)}$ that for the other arm, with $d_j^{(\alpha)}$ the ideal (binary) values. This model has been fit to the phonon spectra of the binary compounds¹⁷ and produces very good agreement between the calculated and observed impurity bond lengths in isovalent alloys.²⁷ Its major deficiencies—the relative insensitivity of the results to additional Coulomb terms¹⁷—will not affect our conclusions on the *relative* stabilities of bulk *versus* epitaxial forms. We use²⁷ $d_{\text{GaP}}^0 = 2.36$ Å, $d_{\text{InP}}^0 = 2.541$ Å, $\alpha_{\text{GaP}} = 47.32$ N/m, $\alpha_{\text{InP}} = 43.04$ N/m, $(\beta/\alpha)_{\text{GaP}} = 0.221$, $(\beta/\alpha)_{\text{InP}} = 0.145$, and $\beta(\text{Ga-P-In}) = 7.817$ N/m. Table II gives the results of our calculation for bulk and epitaxially constrained $\text{Ga}_n\text{In}_{4-n}\text{P}_4$, both for fully relaxed and for partially relaxed structures.

VI. ORDERED PHASES

A. Epitaxial and bulk binary compounds

Bulk-grown (free floating) binary zinc-blende compounds naturally have $\eta = \eta_0 = 1$. Figure 1(a) depicts the

deformation energies of *cubic* GaP and InP ($E[AC, a]$, $E[BC, a]$ of Eq. (6)) as dashed lines. When constrained epitaxially to $a_{\parallel} = a_s$, the relevant deformation energy is $\tilde{E}[AC, a_s]$, $\tilde{E}[BC, a_s]$ of Eq. (25), depicted in Fig. 1(a) as solid curves; the shaded area under them shows the substrate strain energy $W_{ss}(a_s)$ of Eq. (27). Under epitaxial conditions the lattice parameter c changes relative to this bulk value (where $c = a$, or $\eta = \eta_0 = 1$), as shown in Fig. 1(b). Note that η is smaller (larger) than $\eta_0 \equiv 1$ for $a_s > a_{\text{eq}}$ ($a_s < a_{\text{eq}}$). Such variations have been observed experimentally for epitaxially grown alloys, e.g., for³³ $\text{In}_x\text{Ga}_{1-x}\text{As}$ grown on InP.

The obvious distinction between the epitaxial and bulk deformation energy curves in Fig. 1 is their *curvature*. We note the following features: (i) The effective *epitaxial* bulk moduli of the binary compounds [B_{eff} of Eq. (29)] derived from the $\tilde{E}[AC, a_s]$ curves are far smaller than the cubic bulk moduli B (Table II). (ii) The substrate strain $W_{ss}^{(\lambda,n)}(a_s)$ [Eq. (28)] in epitaxial systems is decided by the effective bulk modulus B_{eff} ; this strain [shaded areas in Fig. 1(a)] is considerably smaller than in bulk systems. (iii) GaP has a larger substrate strain energy than InP (since it has a larger B_{eff} ; see Table II). This highlights the basic asymmetry and selectivity of substrate strain effects: GaP on InP has *less* strain than InP on GaP [Figs. 1(a) and 1(b)].

B. Effects of structural parameters on stability of ordered ternary compounds

Figures 2 and 3 give the deformation energies and equilibrium structural parameters (at each a_s) of *epitaxial* ternary systems, and Figs. 4 and 5 give analogous information for *bulk* systems. Note that the deformation energy and lattice parameter *at equilibrium* is the same for bulk and epitaxial systems. (This follows trivially from the fact that a substrate with precisely a lattice constant $a_s = a_{\text{eq}}^{(\lambda,n)}$ will exert no strain on an epitaxial layer.)

Within the strain-only (valence-force-field) description we use, the formation enthalpies $\Delta H^{(n)}$ of all *bulk* ordered compounds are identical with the equilibrium deformation energies, since the strain energies of the constituent binaries are zero in equilibrium; see Eq. (6). The most important qualitative feature of the curves for *bulk* ordered compounds (Figs. 4 and 5) is that the enthalpies of all ordered compounds are positive, i.e., all are *unstable* with respect to decomposition into the binary constituents. While the complete formation enthalpies of ordered compounds may under some circumstances be negative when chemical effects are included [see Sec. V and Eq. (41)], we expect the systematic differences between bulk and epitaxial constraints to be well reproduced within this picture. The formation enthalpies of *epitaxial* compounds are discussed in Sec. VI C.

The following observations can be made on the significance of the different cell-internal degrees of freedom for stabilization of ordered ternary compounds; points (i)–(iv) apply equally to bulk and epitaxial systems at equilibrium, while point (v) contrasts bulk and epitaxial behavior.

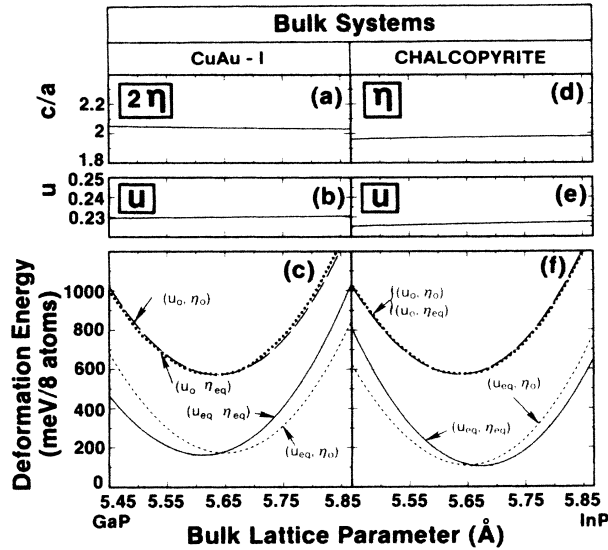


FIG. 4. In analogy with Fig. 2 (see caption), structural parameters and deformation energies for bulk GaInP_2 .

(i) Ternary adamantite compounds $A_nB_{4-n}C_4$ for $n=1,2,3$ are naturally distorted: they exhibit their lowest energies at *distorted* values of both η and $\{u\}$ [see, e.g., the substantial deviations of u_{eq} from $\frac{1}{4}$ in Figs. 4(b), 4(e), and 5(b)]. Interestingly, the dependence on externally controlled cell parameters (the volume, for bulk growth, and the substrate lattice parameter a_s under epitaxial conditions) of equilibrium cell-internal parameters $\{u\}$ is very weak [see, e.g., Figs. 3(b) and 5(b)], while that of η , since it controls cell volume, is much stronger under epitaxial conditions [Figs. 2(a) and 3(a)] than under bulk conditions [Figs. 4(a) and 5(a)].

(ii) Whereas the degeneracy of the strain energy of different structures λ with the same stoichiometry n ap-

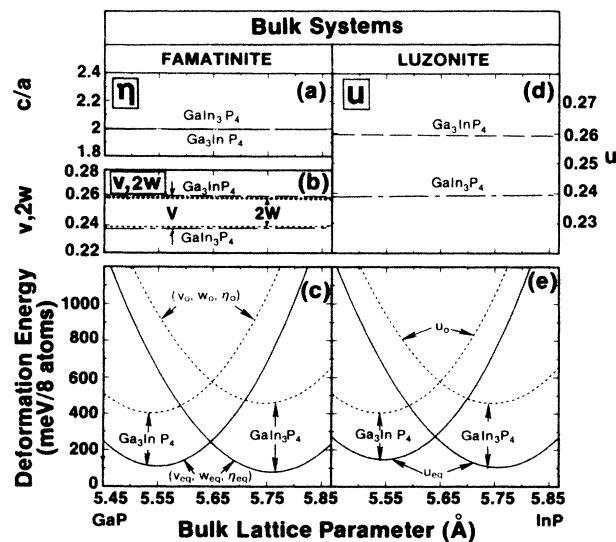


FIG. 5. In analogy with Fig. 3 (see caption), structural parameters and deformation energies for *bulk* GaIn_3P_4 and Ga_3InP_4 .

parent in the *unrelaxed* systems [observe the equal unrelaxed energies $E_{u_0, \eta_0}^{(\lambda, n)}$ of the luzonite-famatinitite (both $n=1$ or 3) and CuAu-chalcopyrite (both $n=2$) pairs in Table II] is removed only slightly in the η -relaxed systems, it is removed completely in the u -relaxed systems. Hence different cell-internal degrees of freedom strongly distinguish among equal-stoichiometry structural pairs. It is apparent from Table II and Figs. 2–5 that while deviations of η from η_0 lower the equilibrium strain energy only marginally, relaxation of the cell-internal degrees of freedom leads to a substantial stabilization of all ternary systems. Moreover, the effects of relaxation of the tetragonal ratio η and cell-internal parameters (u, v, w, \dots) are essentially independent. In Fig. 2, for example, we note that in both the CuAu-I and chalcopyrite structures relaxation of η alone (for $u = u_0$) results in the flattening of the deformation energy curves with respect to the completely unrelaxed case. Relaxation of u alone (for $\eta = \eta_{\text{eq}}$), on the other hand, is responsible for essentially all of the total strain reduction upon relaxation, with essentially no associated flattening of the curves (see Table II). More generally, cell-internal parameters (u, v, w, \dots) control the amount of strain reduction upon relaxation while cell dimensions (η) control the curvature of the energy deformation curves, i.e., equilibrium elastic constants. It follows that the luzonite structure, lacking an η degree of freedom, shows the same effective bulk modulus in both bulk (B) and epitaxial (B_{eff}) forms, whereas all other structures show a considerable reduction of B_{eff} relative to $B^{(n, \lambda)}$ (see Table II). (If we add the η degree of freedom to luzonite, we find the same $\Delta H^{(\lambda, n)}$ values as given in Table II for luzonite, but the $B_{\text{eff}}^{(\lambda, n)}$ values become close to those of famatinitite.)

(iii) The energy lowering upon relaxation reflects the flexibility offered by structural degrees of freedom available. Hence, the luzonite structure with its *two* degrees of freedom $\{a, u\}$ exhibits the smallest energy lowering upon relaxation (-256.2 meV and -353.2 meV for Ga_3InP_4 , and GaIn_3P_4 , respectively), whereas the chalcopyrite structure, with its *three* $\{a, u, \eta\}$ degrees of freedom has the largest energy lowering (by -466.8 meV).

(iv) The relative orientation of the structural parameters can also affect stability: while the chalcopyrite structure accommodates the distinct bond lengths only slightly better than does the CuAu-I structure (since each has two structural degrees of freedom), the difference in strain reduction between the two is mainly due to the differing orientations of the u parameter in each [see insets to Figs. 2(c) and 2(f)]. In the chalcopyrite structure, the strain energy may be minimized with respect to η and u independently since they describe orthogonal distortions [respectively, along the z direction and in the (x, y) plane], while in the CuAu-I structure the two parameters have correlated effects, since both are oriented along z and are hence less effective in reducing strain. Hence, the chalcopyrite shows a larger energy lowering (-466.8 meV) relative to the CuAu-I form (-410.4 meV).

(v) In contrast to the epitaxial case, under bulk growth conditions (Figs. 4 and 5) one finds only a very weak dependence of the tetragonal ratio c/a upon a (V)—

even for structures characterized by a tetragonal unit cell. As a rule under bulk conditions one finds $\eta[a(V)] \simeq \eta(a_{\text{eq}}^{(n)}) \simeq \eta_0$, where η_0 is the tetragonal ratio for the unrelaxed structure, while for epitaxial conditions³⁰ $\eta(a_s) \simeq \eta_0^{(n)} c_{\text{eq}}^{(n)}(a_s)/a_s$ with $c_{\text{eq}}^{(n)}(a_s)$ given in Eq. (33).

We conclude that the availability and orientation of cell-internal structural degrees of freedom—the hallmark of ternary adamantine structures²¹—is the primary mechanism for strain stabilization and phase selectivity (e.g., famatinite over luzonite, chalcopyrite over CuAu-I) in these systems. We will find below that these degrees of freedom are responsible for delicate differences in B_{eff} within competing structures of the same composition (i.e., chalcopyrite and CuAu-I). We turn next to the phase selectivity of epitaxial structures.

C. Stabilization and structural selectivity of epitaxial ternary compounds

Calculating the epitaxial $\delta H^{(\lambda,n)}(a_s)$ of Eq. (26) within the VFF description, we note (Fig. 6) the following features.

(i) The most obvious feature of Fig. 6 is that the epitaxial formation enthalpy $\delta H^{(\lambda,n)}(a_s)$ is *negative* over most of the range $a_{\text{GaP}} < a_s < a_{\text{InP}}$, except for luzonite Ga_3InP_4 , i.e., an ordered ternary compound may be *stable* under *epitaxial* conditions even if *unstable* in *bulk* form. For this phenomenon we will use the term *epitaxial stabilization*. [The simple harmonic model of Eq. (31) and the assumption $B_{\text{eff}}^{(n)} \simeq (n/4)B_{\text{eff}}^{AC} + (4-n)/4B_{\text{eff}}^{BC}$ and $a_{\text{eq}}^{(n)} \simeq (n/4)a_{AC} + (4-n)/4a_{BC}$ (closely obeyed in Table II) semiquantitatively reproduces Fig. 6 for chalcopyrite and famatinite phases (including the relative positions of Ga_3InP_4 and GaIn_3P_4). More subtle features, such as the very different behavior of CuAu-I and chalcopyrite structures under the epitaxial constraint, are associated with delicate deviations from the composition-weighted values for both $a_{\text{eq}}^{(n)}$ and $B_{\text{eff}}^{(n)}$ because of the different structural parameters available.] Epitaxial stabilization effects can explain the observed stability of *epitaxial* adamantine compounds^{4–9} with no counterparts in the *bulk* form.

(ii) Epitaxy-induced strain performs a “natural selection” between different ternary species, preferring the “fittest” (Fig. 6): whereas the luzonite and famatinite forms (or the CuAu-I and chalcopyrite forms) have the same deformation energies in the unrelaxed *bulk* forms (Table II), under *epitaxial* conditions the substrate strain removes this degeneracy, strongly preferring (for all values of a_s) the famatinite (u, v, η degrees of freedom) over the luzonite (just^{22(b)} the u degree of freedom), or the chalcopyrite over the CuAu-I form (for $a_s > 5.53$ Å). In general, phases with the smallest $B_{\text{eff}} a_{\text{eq}}(a_s - a_{\text{eq}})^2$ are favored [Eq. (28)]. This explains why rhombohedral SiGe, with its smaller B_{eff} , grows epitaxially on Si in preference to the zinc-blende phase,³ which is nearly as stable in bulk form but has a larger¹⁶ B_{eff} .

(iii) No obvious condition of “lattice matching” can be associated with the minimum of $\delta H^{(\lambda,n)}(a_s)$ in Fig. 6:

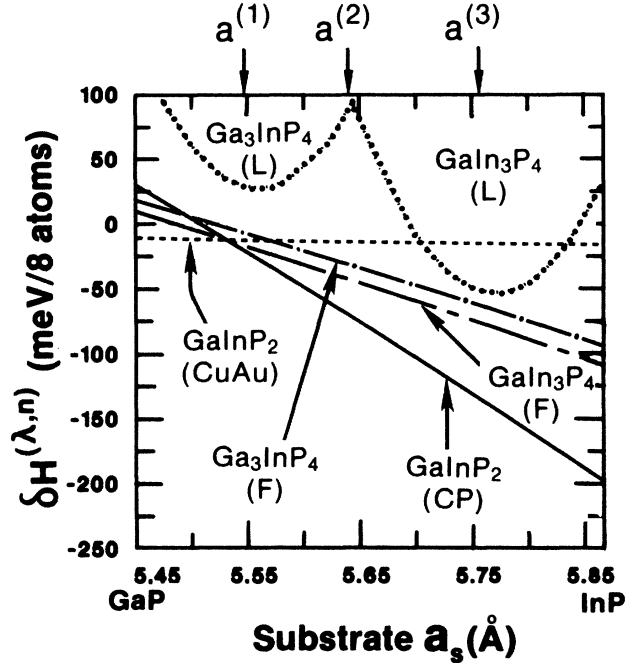


FIG. 6. Enthalpies of formation for epitaxial $\text{Ga}_n\text{In}_{4-n}\text{P}_4$ ordered compounds as a function of the substrate lattice parameter a_s , showing epitaxial stabilization and selectivity.

whereas the energy $E^{(\lambda,n)}(V)$ of the relaxed bulk $A_n B_{4-n} C_4$ system has a minimum at its $a_{\text{eq}}^{(n)}$ (Figs. 2 and 3), the optimum substrate a_s for $\delta H^{(\lambda,n)}(a_s)$ (Fig. 6) is the one that *stabilizes* $A_n B_{4-n} C_4$ and at the same time *destabilizes* its binary constituents most. Hence, the common approach¹⁰ of attempting to match $a_{\text{eq}}^{(n)}$ to a_s diminishes selectivity effects.

(iv) Figure 6 shows that the selection of a substrate with a particular a_s value can alter the relative stabilities of two phases, hence permitting one to grow in preference to the other (e.g., for $a_s < 5.53$ Å the chalcopyrite becomes less stable than the CuAu form).

VII. DISORDERED TERNARY ALLOYS

The average properties of a disordered alloy—either in bulk form or grown epitaxially—may be calculated using the formalism of Secs. III B and IV B. For a random alloy one must decide, in selecting ordered structures whose local clusters are characteristic of the random alloy, how best to represent the alloy. The Landau-Lifshitz structures belonging to the [100] star of ordering vectors include the luzonite structure, which lacks a tetragonal degree of freedom and so offers reduced flexibility in accommodating different $A-C$ and $B-C$ bond lengths. We have therefore used the (2,0,1) ordering vector structures, i.e., famatinite for $A_3 B C_4$ and $A B_3 C_4$ and chalcopyrite for $A_2 B_2 C_4$ (all of which may have $\eta \neq 1$) in evaluating random alloy properties.

A. Bond lengths of bulk disordered alloys

Recent extended x-ray absorption fine structure (EXAFS) experiments³⁴ showed average bond lengths $R_{AC}^D(x)$ and $R_{BC}^D(x)$ in pseudobinary adamantine alloys very close to the corresponding ideal bond lengths d_{AC}^0 and d_{BC}^0 . This behavior has been explained by Martins and Zunger²⁷ on the basis of a structural optimization of a valence force field. This theoretical model also predicted successfully a number of alloy and impurity bond lengths not measured at that time.

We have calculated the concentration variation of the alloy bond lengths of Eq. (24), appropriate for a high-temperature alloy. For each volume $V_{eq}(x)$ we use the fully optimized (η_{eq}, u_{eq}) bond lengths of the ordered structures. These are averaged with the weights of Eq. (18), producing $R_{AC}^D(x)$ and $R_{BC}^D(x)$ depicted in Fig. 7. Figure 7 also shows the values of the ideal bond lengths d_{GaP}^0 and d_{InP}^0 as dashed horizontal lines. The results of Martins and Zunger²⁷ for the dilute impurity limits GaP:In and InP:Ga (solid circles in Fig. 7 labeled MZ) are seen to be in good agreement with our results extrapolated to $x=0$ (for R_{In-P}) and $x=1$ (for R_{Ga-P}). In Fig. 7 the equilibrium bond lengths $R_{AC}^{(n)}$ and $R_{BC}^{(n)}$ for the corresponding ordered phases (zinc blende, chalcopyrite, famatinite) at the stoichiometric compositions $X_n = n/4$ are shown as squares.

Our calculated alloy bond lengths clearly show a bimodal distribution, despite the fact that the $V_{eq}(X)$ which solves Eq. (12) is extremely close, for $Ga_x In_{1-x} P$, to the Vegard rule value $xV_{AC} + (1-x)V_{BC}$. $R_{AC}^D(x)$ and $R_{BC}^D(x)$ are considerably closer to the ideal bond lengths d_{AC}^0 and d_{BC}^0 , respectively, than they are to the concentration weighted average $xd_{AC}^0 + (1-x)d_{BC}^0$. Nevertheless, alloy bond lengths do deviate from the ideal bond lengths, causing residual strain energy and leading to a positive mixing enthalpy $\Delta H^D(x)$ (Fig. 8 below). Note that the bond lengths $R_{AC}^{(n)}$ and $R_{BC}^{(n)}$ of or-

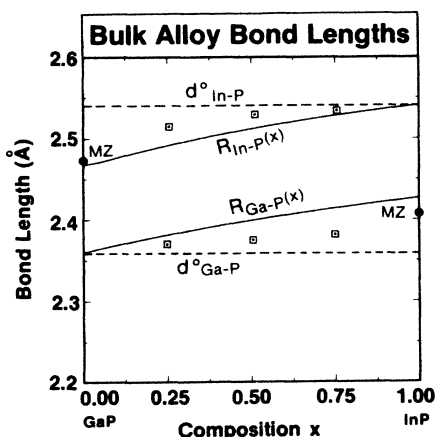


FIG. 7. Ga—P and In—P bond lengths in *bulk* random alloy. Squares indicate ordered phase values for stoichiometric $A_n B_{4-n} C_4$ compounds; MZ indicates values predicted by Martins and Zunger in Ref. 27 from the dilute impurity model. Dashed horizontal lines indicate bond lengths d^0 in the binary systems.

dered structures (squares in Fig. 7) are considerably closer to the ideal values d_{AC}^0 and d_{BC}^0 (dashed lines) than are the bond lengths $R_{AC}^D(X_n)$ and $R_{BC}^D(X_n)$ of the *disordered* alloy at the stoichiometric compositions X_n . This implies²³ that the mixing enthalpy of alloys $[\Delta H^D(X_n)]$ is larger than the formation enthalpy $(\Delta H^{(\lambda, n)})$ of the ordered structures from which the alloy is constructed. The *variety* of local environments (i.e., of A—C and B—C bond lengths) necessitated by disorder in the bulk alloy does not accommodate the distinct bond lengths at concentrations X_n as well as do the *ordered* phases which have each a *single* type of A—C and B—C bond type. In recent work Patrick *et al.*³⁵ and Sher *et al.*³⁶ calculated the bond lengths $R_{Ga-P}(x)$ and $R_{In-P}(x)$ for the disordered $Ga_{1-x} In_x P$ alloy. They attempt to associate their “stiff $\beta=0$ ” model (which exhibits pathological bond lengths nonmonotonic in composition [Fig. 3(b) of Ref. 35]) with that used by Srivastava *et al.*²³ and Mbaye *et al.*,²⁴ i.e., the same description used here, and criticize the validity of the superposition of clusters approach on this basis. In fact, however, our Fig. 7 shows none of the pathologies of their stiff $\beta=0$ model and closely resembles their optimal “relaxed” model [Ref. 35, Fig. 3(a)].

B. Mixing enthalpies of bulk disordered alloy

1. Effects of relaxation of structural parameters

The imperfect accommodation of distinct bond lengths in a disordered alloy has important implications for the enthalpy of mixing $\Delta H^D(x)$ of the bulk alloy. Unfortunately, no direct measurements are available for ΔH^D in semiconductor alloys. Instead, these values are extracted from fits to liquidus-solidus data assuming simple thermodynamic models, and involve a large uncertainty.²⁶ Given this situation, we will proceed as follows. First, we calculate the first two terms (in large

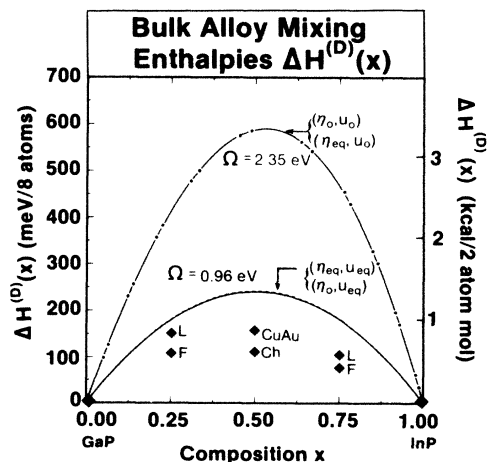


FIG. 8. Mixing enthalpy $\Delta H^D(x)$ [Eq. (13)] for the bulk random $Ga_x In_{1-x} P$ alloy. Chain-dash line indicates unrelaxed structural parameters, solid line fully relaxed. Ω denotes the interaction parameter obtained by fitting the calculated lives of the phenomenological form of Eq. (19).

parentheses) in Eq. (17) using random probabilities and the equation of states [Eq. (8)] for the five ordered phases, keeping $K^b=0$ in both cases. We then examine the effects of alloy-induced cluster relaxation ($K^b \neq 0$).

In Fig. 8 we show the enthalpies of formation of ordered ternary compounds as diamonds, together with results for the disordered bulk alloy. In all cases we note that the mixing enthalpy of the disordered alloy is positive, i.e., it is *unstable* with respect to decomposition into the binary constituents. Using unrelaxed (UR) energies $E_{\eta_0, u_0}^{(\lambda, n)} [V_{\text{eq}}(x)]$ in the expression Eq. (13) we find the upper curve in Fig. 8, approximately parabolic [as suggested by the conventional experimental parametrization of Eq. (19)] with a maximum at $x=0.53$ which can be fit with $\Omega_{\text{UR}} = \Delta H^D / [x(1-x)] \simeq 2.35$ eV/eight atoms or 13.5 kcal per two-atom mole, as determined by a least-squares fit. This agrees very well with the macroscopic model of Fedders and Muller³⁷ (who found $\Omega=13.00$ kcal/mole), but is in substantial disagreement with experiment³⁸ ($\Omega=3.4 \pm 2$ kcal/mole). (Fedders and Muller used an empirically determined multiplicative constant of 0.226 to bring their results for ternary III-V alloys into better agreement with experiment.) To understand the discrepancy with experiment we examine the effects of sequential structural relaxation of the ordered structures on the mixing enthalpy. We find a negligible effect of relaxation of the tetragonal parameter η , because of the very weak dependence of η on volume and its proximity in all cases to the undistorted value (Figs. 4 and 5). Relaxation of cell-internal structural parameters, on the other hand, profoundly affects the enthalpy of mixing. The lowest curve in Fig. 8, corresponding to complete relaxation (denoted R), is almost perfectly parabolic with a maximum at $x=0.503$ and an interaction parameter $\Omega_R=0.961$ eV/eight atoms or 5.54 kcal/mole. This is in considerably better agreement with experiment,³⁸ with the result of Martins and Zunger²⁷ ($\Omega=4.56$ kcal/mole) and with the value obtained from the semiempirical model of Stringfellow²⁶ (3.64 kcal/mole). Since we have neglected chemical interactions [second term in Eq. (41)] in our strain-only model, their inclusion may lower^{23,24} our calculated Ω_R , bringing it into better agreement with experiment. Chen and Sher,³⁹ relaxing constituent clusters as we do, have calculated Ω_R assuming "the size of the tetrahedra for all n clusters at a given alloy concentration takes on the corresponding virtual crystal (i.e., Vegard rule) value, but allowing the central C atom to relax." Though no numerical results were given, they concluded that "the energies are too large and would correspond to Ω_R values many times the experimental values."³⁹ Our result ($\Omega_R=5.54$ kcal/mole versus $\Omega_{\text{exp}}=3.4 \pm 2$ kcal/mole), and the similarity of both approaches, demonstrates that their calculation must have been in error.

2. Effects of alloy-induced cluster relaxation

In the notation of Eqs. (20)–(23) we have found that structural parameters are completely unrelaxed

$$\Omega_1^{\text{UR}} = 9.9 \text{ kcal/mole}, \quad (43)$$

while if η and $\{u\}$ are relaxed (R)

$$\Omega_1^R = 2.02 \text{ kcal/mole}. \quad (44)$$

The cluster strain contribution [Ω_2 of Eq. (22)] is insensitive to structural relaxation, yielding

$$\Omega_2^{\text{UR}} = 3.6 \text{ kcal/mole}, \quad \Omega_2^R = 3.5 \text{ kcal/mole}. \quad (45)$$

We may write the total interaction parameter of Eq. (20) as

$$\Omega = (\Omega_1^{\text{UR}} + \Omega_2^{\text{UR}}) + [(\Omega_1^R - \Omega_1^{\text{UR}}) + (\Omega_2^R - \Omega_2^{\text{UR}})] + \Omega_3. \quad (46)$$

The second and third terms give, respectively, the reduction in Ω due to relaxation of structural parameters and due to alloy-induced cluster relaxation. Since our result neglecting alloy-induced cluster relaxation $\Omega_1^R + \Omega_2^R$ falls within the large error bars for the observed Ω , it is difficult to quantitatively assess K^b . In metallurgical systems, for which $\Delta H^D(x, T)$ is measured directly and accurately, a similar calculation²⁵ for $\text{Cu}_x\text{Au}_{1-x}$ yielded a modest relaxation constant of $K \simeq 0.21$. We can determine the *range* of K consistent with the experimental value for Ω for $\text{Ga}_x\text{In}_{1-x}\text{P}$ by equating the calculated $\Delta H^D/x(1-x)$ of Eq. (19) with the mean experimental value of 3.4 ± 2 kcal/mole. We find $K^b=0.37$, and hence $\Omega_3 = -2.1 \pm 2$ kcal/mole.

Since $\Omega_1^{\text{UR}} + \Omega_2^{\text{UR}} = 13.5$ kcal/mole and structural relaxation reduces Ω by 8.0 kcal/mole, we conclude that (i) relaxation of structural parameters in the ordered compounds used to describe the disordered alloy (mostly the cell-internal parameters $\{u\}$ which control the accommodation of distinct $A-C$ and $B-C$ bond lengths) is the most important energy-lowering mechanism. (We may infer that the phenomenological factor of 0.226 Fedders and Muller³⁷ used to make their theoretical predictions for Ω agree with experiment accounts mainly for structural relaxation.) (ii) The contribution Ω_1^R of the bulk formation enthalpies and that from alloy-induced cluster relaxation Ω_3 tend to cancel, making $\Delta H^D(x) \simeq h_{\text{bulk}}^D(x) = \Omega_2^R x(1-x)$ a reasonable approximation. Ferreira *et al.*⁴⁰ have justified such an approximation from different considerations, which predict that $\Omega_2^{\text{UR}} \simeq (\Omega_1^{\text{UR}} + \Omega_2^{\text{UR}})/4$, i.e., that the true interaction parameter is about one-fourth that of the completely unrelaxed (Fedders-Muller) value, in reasonable agreement with our result $(\Omega_1^{\text{UR}} + \Omega_2^{\text{UR}})/\Omega_2^{\text{UR}} \simeq 3.7$. (iii) Alloy-induced cluster relaxation will lower Ω further, and (iv) ordered $A_n B_{4-n} C_4$ compounds of lattice-mismatched compounds AC and BC have a lower formation enthalpy $\Delta H^{(n)}$ (diamonds in Fig. 8) than the mixing enthalpy of a disordered alloy of the same composition, because of the better accommodation of distinct bond lengths in the pure compound environment (versus the variety of environments statistically mandated in the disordered alloy).

C. Bond lengths of epitaxial disordered alloys

In Fig. 9 we show the alloy-averaged Ga—P and In—P bond lengths for epitaxial $\text{Ga}_{1-x}\text{In}_x\text{P}$ and those for

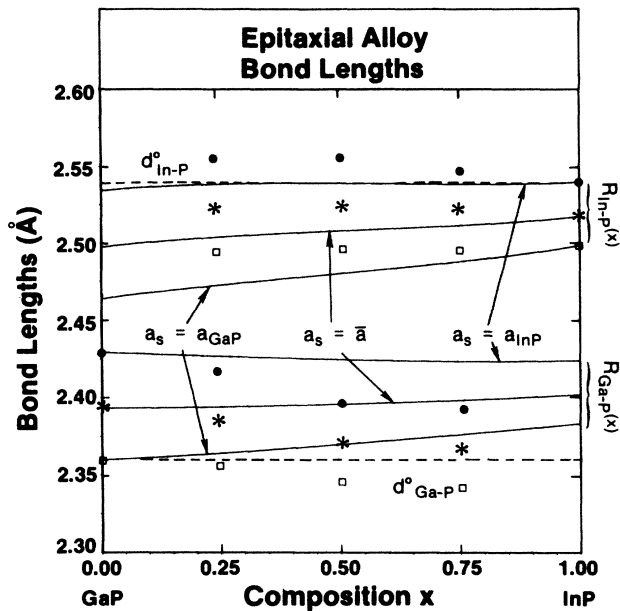


FIG. 9. In analogy with Fig. 7 (see caption), bond lengths for the epitaxial random $\text{Ga}_x\text{In}_{1-x}\text{P}$ alloy and ordered compounds for substrate lattice parameters $a_s = a_{\text{GaP}}$ [5.45 Å (squares)], $\bar{a} = (a_{\text{GaP}} + a_{\text{InP}})/2 = 5.65$ Å (asterisks), and $a_{\text{InP}} = 5.868$ Å (solid circles).

ordered epitaxial compounds at the stoichiometric compositions for the same substrate lattice parameters.⁴¹

As in the bulk case of Fig. 7, the epitaxial disordered alloy shows a bimodal bond length distribution. Ga—P and In—P bond lengths for bulk ordered compounds are monotonic across the sequence $n = 0-4$; under epitaxial conditions [at fixed a_s , but at $c_{\text{eq}}^{(n)}(a_s)$; see Eq. (33)] they are also monotonic across this series (squares in Fig. 9 for fixed substrate), except for $R(\text{Ga—P})$ for $a_s = a_{\text{GaP}}$ and for $R(\text{In—P})$ for $a_s = a_{\text{InP}}$. This is yet another manifestation of the extreme selectivity between ordered structures associated with epitaxial growth and a reflection of the differing numbers of structural parameters available to each (2,0,1) structure (for fixed a_s , one for the binaries, three for farnite, two for chalcopyrite). These fluctuations are not apparent in the bond lengths for the alloy. The ideal bond Ga—P and In—P bond lengths are shown as horizontal dashed lines. It is apparent, as in the bulk case, that Ga—P and In—P bond lengths in the disordered alloy lie farther from the ideal values than the corresponding bond lengths in epitaxial ordered $\text{Ga}_n\text{In}_{4-n}\text{P}_4$ compounds, except for Ga—P bond lengths for $a_s = a_{\text{GaP}}$ and for In—P bond lengths for $a_s = a_{\text{InP}}$.

D. Mixing enthalpies of epitaxial disordered alloys

Finally, we show in Figs. 10(a) and 10(b) the epitaxial mixing enthalpy $\delta H^D(x, a_s)$ of Eq. (38) measured with respect to strained binary compounds (i.e., with $a_{\parallel} = a_s$). For convenience in evaluating $c_{\text{eq}}(x)$, shown in Fig. 10(c), we have used a harmonic approximation in describing all cluster properties. Compared with the bulk value $\Delta H^D(x)$ of Fig. 8 (positive for all x 's), we

Epitaxial Alloy Mixing Enthalpy $\delta H^D(x, a_s)$

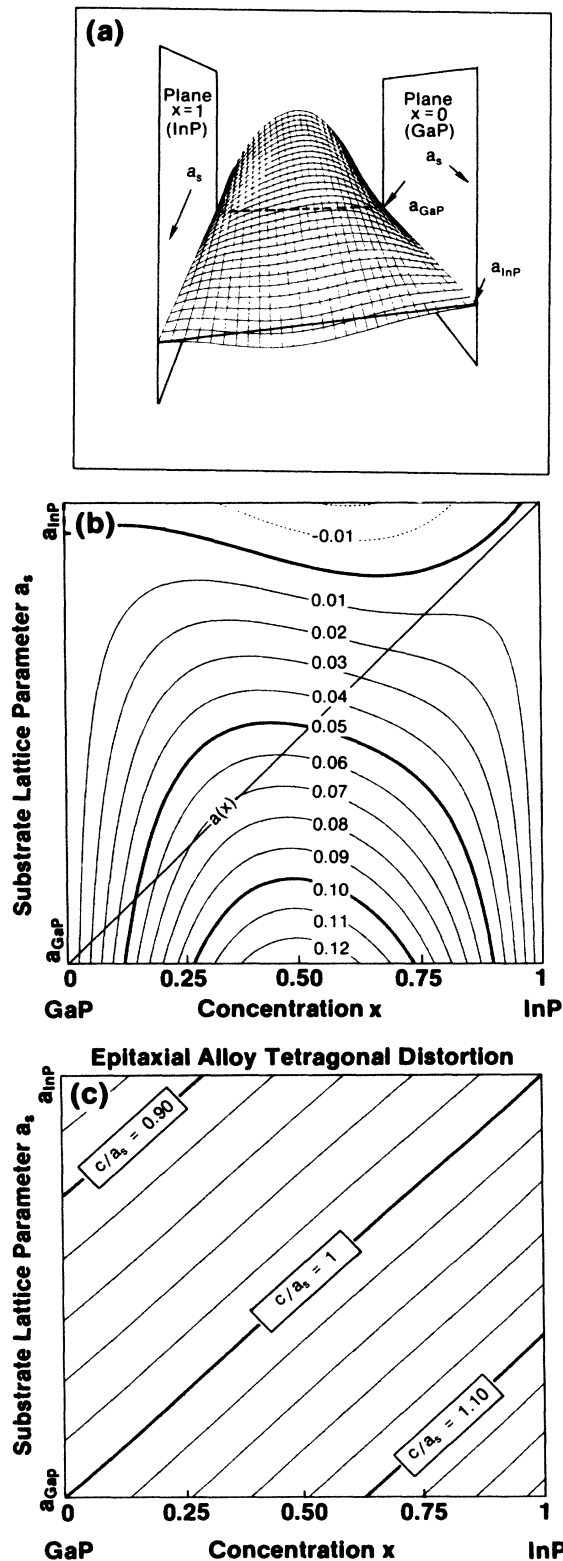


FIG. 10. Mixing enthalpy of epitaxial $\text{Ga}_{1-x}\text{In}_x\text{P}$ random alloy with respect to strained disproportionation products [Eq. (38)], (a) and (b), and epitaxy-induced alloy tetragonal distortion, $c_{\text{eq}}(a_s, x)/a_s$, (c). Contour levels in (b) are in eV/eight atoms, where the solid diagonal line depicts the average (Vegard) lattice parameter $a(x)$ of the alloy.

note two important features, one qualitative and one quantitative.

(i) the *epitaxial* mixing enthalpy can be negative, hence even the *disordered* alloy may become *stable* under epitaxial conditions. When the substrate lattice parameter a_s is close to that of GaP, the epitaxial alloy is unstable [$\delta H^D(x) > 0$], qualitatively like its bulk alloy counterpart. For a_s near a_{InP} , however, the entire composition range becomes stable. This reflects the fact that an epitaxial system, unlike its bulk counterpart, becomes more stable as the disproportionation products ($AC + BC$) are more strained. If one alloy constituent (here GaP) is significantly stiffer (compare the bulk moduli in Table II) than the other (InP), selecting a substrate with a_s very different from its own natural a_{AC} leads to a substantial strain of the disproportionation product AC , thus stabilizing the alloy *against* disproportionation.

(ii) Of two important quantitative features of Fig. 10, we note first that, (a) values of $\delta H^D(a_s, x)$ in Fig. 10(b) are much smaller than corresponding values of $\Delta H^D(x)$ in Fig. 8. As an example, we note that along the “Vegard rule” line readily accessible experimentally [diagonal line in Fig. 10(b)] δH^D is no larger than about 70 meV per eight atoms across the entire composition range for epitaxial $\text{Ga}_x\text{In}_{1-x}\text{P}$, while for the bulk alloy ΔH^D (lower curves in Fig. 8) it can be as high as 250 meV per eight atoms across this range. This large reduction of the mixing enthalpy implies that the miscibility gap temperature of epitaxial alloys will be reduced relative to that of bulk alloys.¹⁵ Secondly, (b) despite the stabilization of the *disordered* alloy by epitaxial growth, *ordered* compounds remain yet more stable, since the “ordering energy”

$$\Delta E_{\text{ord}}(a_s) \equiv \delta H^{(n)}(a_s, X_n) - \delta H^D(a_s, X_n)$$

depends relatively weakly on a_s and is strictly negative for famatinite Ga_3InP_4 and GaIn_3P_4 and chalcopyrite $\text{Ga}_2\text{In}_2\text{P}_4$. Thus provided $\delta H^{(n)}(a_s) < 0$, the ordered phases will be more stable than the disordered.

This result implies a novel approach to material engineering of pseudomorphic epitaxial ordered or disordered systems, best illustrated by a particular example. Suppose a 50%-50% alloy is grown epitaxially on a substrate with a_s . The solid diagonal line in Fig. 10(b) depicts the average (Vegard) alloy lattice parameter $a(x)$. The common practice in crystal growth is to select a substrate whose a_s best matches the alloy lattice parameter $a_{\text{eq}}(x)$ at the chosen composition [$a_{\text{eq}}(0.5)$ in our particular example]. Figure 10(c) shows that this choice guarantees no average epitaxy-induced strain in the alloy [$c_{\text{eq}}(a_s, x)/a_s \approx 1$]. Figure 10(b) shows, however, that $\delta H^D(0.5, a_s)$ could be further lowered if a_s were selected to be *larger* than $a_{\text{eq}}(0.5)$, provided the growth is still pseudomorphic. In actuality, the lattice mismatch $|a_s - a_{\text{eq}}(x)|$ sets up a strain energy²⁸ which would induce misfit dislocations beyond a critical mismatch; only layers of a limited thickness $h < h_c[a_s - a_{\text{eq}}(x)]$ could then be grown dislocation-free. This suggests that, if one were content with such thin layers, there would be a definite thermodynamic *advantage* to select a *large*

mismatch $|a_s - a_{\text{eq}}(x)|$.

The preceding discussion of stability of alloys has utilized the *random* probabilities $P_R^{(n)}(x)$ [Eq. (18)]. More refined calculations²⁴ indicate that substantial nonrandomness can exist. We therefore wish to point out that generation of misfit dislocations is not the sole mechanism for relieving substrate-epilayer strain. The epitaxial alloy could, alternatively, reduce this strain by *enhancing* the occurrence probabilities $P^{(n)}(x, T)$ (in excess of those granted by random distributions) of the fittest species n at a given x [i.e., those that, according to Figs. 2 and 3, are least strained at this $a(x)$], and conversely, *reducing* $P^{(n)}(x, T)$ of the most strained species. This mechanism of “natural selection of species” will have to be included in more traditional models of misfit dislocations²⁸ to obtain better approximations to the critical layer thickness h_c of disordered epitaxial alloys.

VIII. SUMMARY AND CONCLUSIONS

The Landau-Lifshitz theory of structural phase transitions permits identification of likely candidates for ordered ternary structures in the phase diagrams of $A_xB_{1-x}C$ pseudobinary alloys. We have presented in detail a prescription for how disordered alloys may be quantitatively described as a temperature- and composition-dependent superposition of local tetrahedral environments found within the ordered phases. The structural properties of bulk and epitaxial disordered $\text{Ga}_x\text{In}_{1-x}\text{P}$ alloys were determined variationally and the enthalpy of formation and bond lengths for bulk and epitaxial alloys were examined.

Our conclusions are as follows.

(i) The hallmark of ordered ternary adamantite $A_nB_{4-n}C_4$ compounds is the existence of cell-internal structural parameters (which control the $A-C$ and $B-C$ bond lengths and angles), in addition to the usual, cell dimensions. Different $A_nB_{4-n}C_4$ structures are distinguished by the number and orientation of the cell-internal degrees of freedom [Eqs. (1)–(4)]. The bulk binary (AC and BC) zinc-blende constituents have only one degree of freedom (the cubic lattice parameter).

(ii) Ordered compounds nevertheless cannot make all bond angles exactly tetrahedral and all bond lengths equal their binary values.¹⁶ This imperfect accommodations results in “frozen-in” microscopic strain energy.

(iii) Even under bulk conditions, $A_nB_{4-n}C_4$ compounds having the same stoichiometry but different crystal structures (e.g., the famatinite-luzonite pair for A_3BC_4 , or the chalcopyrite-CuAu-I pair for ABC_2) have distinctly different microscopic strain energies, due to the different number and orientations of cell-internal degrees of freedom ($\Delta H^{(n)}$ in Table II). Although the strain energies within each pair are identical when the structural parameters are unrelaxed, relaxation of these degrees of freedom stabilizes, e.g., famatinite (with two cell-internal degrees of freedom) over luzonite (a single cell-internal degree of freedom), and chalcopyrite (two orientationally independent degrees of freedom) over the CuAu-I-like structure (two directionally correlated degrees of freedom).

(iv) Under pseudomorphic epitaxial growth conditions, one degree of freedom—the cell dimension parallel to the substrate—is externally fixed. This results in “substrate strain energy” [Eq. (27)]. Relative epitaxial stability of different structures is then determined by the ability of the system to lower its strain through relaxation of the remaining degrees of freedom. While binary AC or BC compounds can do so only by tetragonally deforming (Fig. 1), ternary systems can also utilize their cell-internal degrees of freedom to lower their epitaxy-induced strain energies (Figs. 2 and 3).

(v) Epitaxial pseudomorphic growth of an ordered compound on a substrate with lattice parameter a_s results in considerably flatter $\tilde{E}(a_s)$ curves (Figs. 2 and 3) relative to the $E(a)$ curve for bulk growth (Figs. 4 and 5). This elastic softening (by a factor B_{eff}/B where B_{eff} depends on the substrate orientation and B is the bulk modulus) reflects the availability of a tetragonal degree of freedom. Since different compounds have different B_{eff} values, one can be epitaxially stabilized over another even if both have the same equilibrium lattice constant (“epitaxial selectivity”). Hence, rhombohedral SiGe with its smaller B_{eff} grows epitaxially on Si in an ordered fashion, whereas the zinc-blende phase of SiGe, with its larger B_{eff} , does not.^{3,16}

(vi) While the epitaxial restriction $a_{\parallel} = a_s$ necessarily raises the energies of AC , BC , and $A_nB_{4-n}C_4$ relative to the equilibrium values, it frequently occurs, because of

(iv) and (v) above, that the epitaxial constraint destabilizes the binary constituents AC and BC even more than that of $A_nB_{4-n}C_4$. Consequently, an ordered epitaxial compound (Fig. 6) can be stable even if it was unstable in bulk form, hence epitaxial stabilization. Epitaxial phases with no bulk counterparts may hence exist.^{4–9} Furthermore, substrate strain performs a natural selection between ternary species, preferring the fittest (the one whose cell-internal degrees of freedom make it most adaptable to the substrate). Thus, e.g., chalcopyrite is favored epitaxially over CuAu-I (Fig. 6).

(vii) The mixing enthalpy of bulk isovalent disordered alloys $A_xB_{1-x}C$ is expected generally to be positive (Fig. 8) even if formation enthalpies of the ordered $A_nB_{4-n}C_4$ compounds are slightly negative.²⁶ This is so, for appreciable lattice mismatch between the constituents, because the variety of local atomic environments necessitated by disorder does not accommodate the distinct bond lengths and bond angles as well as do the ordered phases, which have each a single type of local bond configuration (Fig. 7). In contrast, the epitaxial constraint stabilizes disordered alloys (thus depressing miscibility gap temperatures) and may even make the mixing enthalpy negative for some substrates.

(viii) Ordered compounds are nonetheless stabilized more by the epitaxial constraint than are disordered alloys.

*Permanent address: Laboratoire de Physique du Solide et Energie Solaire, Centre National de la Recherche Scientifique, 06560 Valbonne, France.

¹See, for example, *Structure and Bonding in Crystals*, edited by M. O’Keeffe and A. Navrotsky (Academic Press, New York, 1981), Vols. I and II.

²P. Villars and L. D. Calvert, *Pearson’s Handbook of Crystallographic Data for Intermetallic Phases* (American Society for Metals, Ohio, 1985).

³(a) A. Ourmazd and J. C. Bean, *Phys. Rev. Lett.* **55**, 765 (1985); (b) S. Mahajan, D. E. Laughlin, and H. M. Cox, *ibid.* **58**, 2567 (1987).

⁴H. Nakayama and H. Fujita, in *GaAs and Related Compounds 1985* (Karuizawa, Japan, 1986), p. 289.

⁵H. R. Jen, M. J. Cherng, and G. B. Stringfellow, *Appl. Phys. Lett.* **48**, 1603 (1986).

⁶(a) T. S. Kuan, T. F. Kuech, W. I. Wang, and E. L. Wilkie, *Phys. Rev. Lett.* **54**, 210 (1985); (b) T. S. Kuan, W. I. Wang, and E. L. Wilkie, *Appl. Phys. Lett.* **51**, 51 (1987).

⁷M. Bujatti, *Phys. Lett.* **24A**, 36 (1967).

⁸S. Nishino, Y. Kazuki, H. Matsunami, and T. Tanaka, *J. Electrochem. Soc.* **124**, 2674 (1980).

⁹R. Ritz and H. Lüth, *Phys. Rev. B* **32**, 6596 (1985); M. Matern and H. Lüth, *Surf. Sci.* **126**, 502 (1983).

¹⁰G. B. Stringfellow, *J. Appl. Phys.* **43**, 3455 (1972); M. Quillec, C. Daguët, J. L. Benchimol, and H. Launois, *Appl. Phys. Lett.* **40**, 325 (1982); R. E. Nahory, M. A. Pollack, E. D. Beebe, J. C. DeWinter, and M. Ilegems, *J. Electrochem. Soc.* **125**, 1053 (1978).

¹¹R. M. Cohen, M. M. Cherng, R. E. Benner, and G. B. Stringfellow, *J. Appl. Phys.* **57**, 4817 (1985).

¹²C. Rau, C. Schneider, G. Xing, and K. Jamison, *Phys. Rev. Lett.* **57**, 3221 (1986); M. Onellion, M. A. Thompson, J. L. Erskine, C. B. Duke, and A. Paton, *Surf. Sci.* **179**, 219 (1987).

¹³Z. Q. Wang, Y. S. Li, F. Jona, and P. M. Marcus, *Solid State Commun.* **61**, 623 (1987).

¹⁴(a) D. Pescia, G. Zampieri, M. Stampanoni, G. L. Bona, R. F. Willis, and F. Meier, *Phys. Rev. Lett.* **58**, 933 (1987); (b) G. A. Prinz, *ibid.* **54**, 1051 (1985); (c) V. Yu Aristov, I. L. Bolotin, and V. A. Grazhulis, *JETP Lett.* **45**, 63 (1987).

¹⁵B. de Cremoux, *J. Phys. (Paris) Colloq.* **12**, C5-19 (1982); B. de Cremoux, P. Hirtz and J. Ricciardi, *GaAs and Related Compounds 1980* (The Institute of Physics, Bristol, 1981), p. 115.

¹⁶J. L. Martins and A. Zunger, *Phys. Rev. Lett.* **56**, 1400 (1986).

¹⁷P. N. Keating, *Phys. Rev.* **145**, 637 (1966). See also R. M. Martin, *Phys. Rev. B* **1**, 4005 (1970).

¹⁸A. A. Mbaye, A. Zunger, and D. M. Wood, *Appl. Phys. Lett.* **49**, 782 (1986).

¹⁹L. D. Landau and E. M. Lifshitz, *Statistical Physics* (Pergamon, Oxford, 1969), Chap. 14.

²⁰J. L. Martins and A. Zunger, *J. Mater. Res.* **1**, 523 (1986).

²¹E. Parthé, *Cristallographie des Structures Tetraedriques* (Gordon & Breach, Paris, 1972).

²²There seems to be a controversy in the literature as to the exact structure of Cu_3AsS_4 , often termed luzonite. Some authors believe that the structure we term luzonite [Table I and Eq. (3)] is actually that of the mineral Cu_3VS_4 (“sulvanite,” space group $P\bar{4}3m$), see F. J. Trojer, *Am. Miner.* **51**, 890 (1966), and that the structure we term famatinite is actu-

- ally that of Cu_3AsS_4 ; see F. Marumo, and W. Nowachi, *Z. Krist.* **124**, 1 (1967). To avoid confusion, we specify in Table I and Eqs. (1)–(4) what we mean by these structures; the reader should, however, be aware of the possible uncertainty in assigning the mineral names luzonite and famatinite to these space groups. We thank Dr. D. Cahen for discussing these points with us.
- ²³G. P. Srivastava, J. L. Martins, and A. Zunger, *Phys. Rev. B* **31**, 2561 (1985).
- ²⁴A. A. Mbaye, L. G. Ferreira, and A. Zunger, *Phys. Rev. Lett.* **58**, 49 (1987).
- ²⁵S.-H. Wei, A. A. Mbaye, L. G. Ferreira, and A. Zunger, *Phys. Rev. B* **36**, 4163 (1987).
- ²⁶G. B. Stringfellow, *J. Cryst. Growth* **27**, 21 (1974).
- ²⁷J. L. Martins and A. Zunger, *Phys. Rev. B* **30**, 6217 (1984).
- ²⁸J. H. Van der Merwe, *J. Appl. Phys.* **34**, 123 (1962); J. W. Matthews, S. Mader, and T. B. Light, *ibid.* **41**, 3800 (1970).
- ²⁹For the [111] orientation, the corresponding elastic modulus [see B. de Cremoux, *J. Phys. (Paris) Colloq.* **43**, C5 (1982)] is $\sigma_{111} = 6[4/(C_{11} + 2C_{12}) + 1/C_{44}]^{-1}$. See also W. A. Brantley, *J. Appl. Phys.* **44**, 534 (1973).
- ³⁰For convenience, we adopt a quasicubic harmonic description in which the ordered tetragonal ternary compounds are characterized by $\Delta H^{(n)}$ and the elastic constants C_{11}^{eff} and C_{12}^{eff} , found from the quantities $B^{(n)}$ and $B_{\text{eff}}^{(n)}$ in Table II, thereby omitting relative corrections of order $(C_{33}/C_{11} - 1)$. We also assume that at the global equilibrium $c_{\text{eq}}^{(n)}/a_{\text{eq}}^{(n)} = \eta_0$ (a good approximation, as may be seen from Table II). Comparison of this description with direct valence-force-field calculations suggest that resulting strain energy errors are of order 6% for $\text{Ga}_x\text{In}_{1-x}\text{P}$.
- ³¹See D. M. Wood, S.-H. Wei, and A. Zunger, *Phys. Rev. Lett.* **58**, 1123 (1987); *Phys. Rev. B* **36**, 1342 (1987), and references therein.
- ³²S.-H. Wei, A. Zunger, *Phys. Rev. Lett.* **56**, 2391 (1986).
- ³³M. C. Joncour, J. L. Benchimol, J. Burgeat and M. Quillec, *J. Phys. (Paris) Colloq.* **C-5**, 3 (1982).
- ³⁴J. C. Mikkelsen and J. B. Boyce, *Phys. Rev. Lett.* **49**, 1412 (1982).
- ³⁵R. Patrick, A.-B. Chen, and A. Sher, *Phys. Rev. B* **36**, 6585 (1987).
- ³⁶A. Sher, M. Van Schilfgaarde, A. B. Chen, and W. Chen, *Phys. Rev. B* [In press].
- ³⁷P. A. Fedders and M. W. Muller, *J. Phys. Chem. Solids* **45**, 685 (1984).
- ³⁸I. V. Bondar, E. E. Matyas, and L. A. Makovetskaya, *Phys. Status Solidi A* **36**, K141 (1976).
- ³⁹A. B. Chen and A. Sher, *Mater. Res. Soc. Proc.* **46**, 137 (1985). These authors (private communication) have acknowledged these calculations to be preliminary.
- ⁴⁰L. G. Ferreira, A. A. Mbaye, and A. Zunger, *Phys. Rev. B* (to be published).
- ⁴¹The variation with the tetragonal dimension c of the cell-internal structural parameters $\{u, v, w, \dots\}$ is weak enough (Figs. 2 and 3) that they may be kept fixed at their values at $c_{\text{eq}}^{(n)}$, yielding bond lengths for the ordered compounds which deviate from completely relaxed full valence-force-field calculations by typically less than 0.004 Å. We hence used a quasicubic description (see Ref. 30) and the harmonic model predictions [Eq. (37) for $c_{\text{eq}}(a_s, x)$] in Eqs. (2) and (4) [with $\eta = 2c_{\text{eq}}(a_s, x)/a_s$] for $R_{\alpha\beta}^{(n)}(a_s, c_{\text{eq}})$.

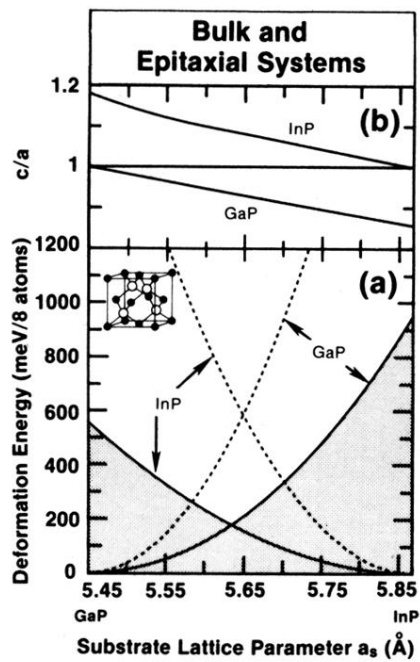


FIG. 1. Deformation energy of cubic (dashed lines) and tetragonally distorted epitaxial (solid lines) GaP and InP, (a), and dependence of c/a upon substrate lattice parameter a_s , (b). Shaded area indicates substrate strain. The inset shows the zinc-blende structure.

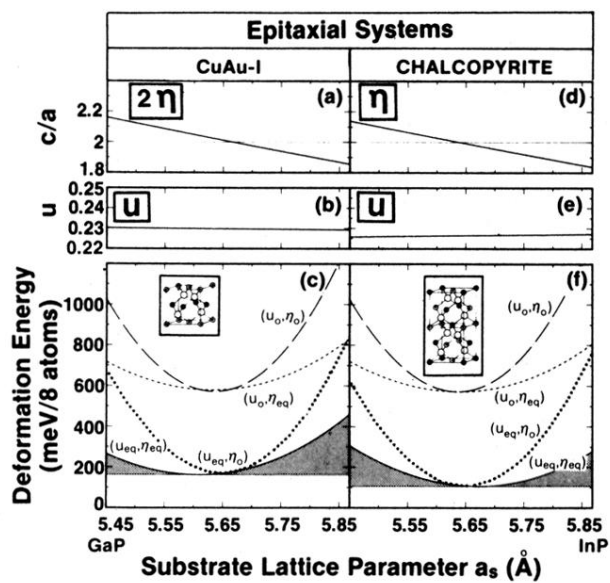


FIG. 2. Variation with substrate lattice parameter of structural parameters and deformation energies of *epitaxial* chalcopyrite and CuAu-I-like GaInP₂; insets show crystal structures. Deformation energies are shown for four different levels of relaxation: subscripts 0 and eq indicate undistorted and fully relaxed values, respectively. Shaded areas indicate substrate strain in the fully relaxed structures.